VISCOELASTIC POLYMER-ASSISTED MECHANICAL EXFOLIATION OF LARGE AREA HIGHLY ORIENTED PYROLYTIC GRAPHITE

A Thesis
Presented to
The Academic Faculty

By

David Hahn

In Partial Fulfillment
Of the Requirements for the Degree
Master in Science in the
School of Mechanical Engineering

Georgia Institute of Technology
May 2017

VISCOELASTIC POLYMER-ASSISTED MECHANICAL EXFOLIATION OF LARGE AREA HIGHLY ORIENTED PYROLYTIC GRAPHITE

Approved by:

Dr. Shreyes Melkote, Advisor
School of Mechanical Engineering
Georgia Institute of Technology

Dr. Christopher Saldana
School of Mechanical Engineering
Georgia Institute of Technology

Dr. Zhigang Jiang
School of Physics
Georgia Institute of Technology

ACKNOWLEDGEMENTS

First of all, I would like to thank Dr. Melkote with endless support and critical advice for both research and life as an advisor. I am indebted for all his sincere feedbacks which motivated me to pursue this academic goal. I would additionally like to thank his Morris M. Bryan, Jr. Professorship for funding this project.

I would also like to thank and acknowledge Dr. Jiang and Dr. Saldana for being the other members of my committee. I would especially like to emphasize my gratitude toward Dr. Jiang, as he and his student, Yuxuan Jiang, collaborated on this project on sharing ideas about more efficiently performing this research and characterizing the exfoliated graphite/graphene sheets, specifically using Raman Spectroscopy and electrical property measurement method.

I want to thank Heat Lab at Georgia Tech and the research engineer Tom Bougher for performing thermal property measurement on the exfoliated graphite sheets obtained in this thesis work.

I would like to express my sincere gratitude to those who shared their knowledge and skills that pushed this research forward. Staffs in the Institute for Electronics and Nanotechnology (IEN), namely Hang Chen, Vinh Nguyen, and Scott Claudon, assisted and trained me to utilize the cleanroom tools for etching the graphite source and characterizing the exfoliated sheets. I would like to thank my lab mates in PMRC, especially Arkadeep Kumar and Pushparghya Kuila, for guiding me to use other important tools like various microscopes and profilometers.

I would also like to give huge thanks to my family in Korea and friends who kept me strong when I was going through difficult times. I would never have completed this research without their continuous support.

TABLE OF CONTENTS

LIST OF TABLES

LIST OF FIGURES

LIST OF SYMBOLS AND ABBREVIATIONS

2-D	two dimensional
HOPG	highly oriented pyrolytic graphite
NEMS	nano-electromechanical systems
PGS	pyrolytic graphite sheets
PEMFC	proton exchange membrane fuel cell
CVD	chemical vapor deposition
MBE	molecular beam epitaxy
PDMS	polydimethylsiloxane
TDTR	time domain thermoreflectance
PVD	physical vapor deposition
CNT	carbon nanotube
AFM	atomic force microscopy
MEMS	micro-electromechanical systems
DOE	design of experiment
S_a	arithmetic surface roughness
PECVD	plasma-enhanced chemical vapor deposition
RIE	reactive ion etching
ICP	inductively coupled plasma
AOE	advanced oxide etch
sccm	standard cubic centimeter per minute

SUMMARY

There is a growing demand for a cost-effective, scalable, and reliable production method for 2D van der Waals materials like graphene and pyrolytic graphite sheets. None of the existing mechanical exfoliation based production methods can reliably produce these materials in large area, high quality, and high yield by mechanically controlling the thickness of the layers exfoliated from the bulk source. Each widely known production/synthesis method for graphene, like the scotch-tape based cleaving method and chemical vapor deposition (CVD), has its own significant limitations, such as low yield and graphene layers with low carrier mobility, respectively. This thesis seeks to overcome these limitations by proposing a new method for controlled mechanical exfoliation of bulk graphite using the adhesive properties of a polydimethylsiloxane (PDMS) stamp.

This thesis describes research conducted to evaluate the capabilities of the PDMS stamp based method to exfoliate large area, thin, high quality graphite sheets from bulk graphite. Experiments were performed to determine the optimum curing time for producing a PDMS stamp with suitable adhesion and stiffness, and to determine the optimum thickness of the PDMS stamp necessary to exfoliate large area and thin graphite sheets with fewer surface defects from a bulk highly oriented pyrolytic graphite (HOPG) source. The effect of roughness of the initial HOPG surface on the exfoliation process was also studied. The results show that graphite sheets with fewer surface defects can be exfoliated by the PDMS stamp if the initial HOPG surface is very smooth. A novel set of experiments were performed to investigate the effect of superposing small amplitude, high frequency oscillation in the shear direction on the PDMS based mechanical exfoliation process. The objective of this experiment was to investigate if the superposition of high frequency oscillation on the regular exfoliation process produces thinner exfoliations. The results

of this experiment show that thinner graphite sheets are produced in the presence of high frequency shear oscillation. The final experiment in this research consisted of evaluating the combined effects of high frequency shear oscillation and the optimum PDMS stamp properties (thickness, surface roughness) on the exfoliation process. The results of this experiment yielded the thinnest, large area graphite sheets. Preliminary scalability of the mechanical exfoliation process was also investigated to qualitatively show that this process is potentially scalable and capable of producing even thinner layers.

Electrical and thermal characterizations of the thinnest exfoliated graphite sheets confirmed that these sheets are electrically and thermally more conductive than commercially available pyrolytic graphite sheets (PGS). These exfoliated graphite sheets are thinner and of higher quality (no D-peak in the Raman spectra). These characterization results, along with the systematic experiments and quantitative studies involving various process conditions and parameters, provide the foundation for further development and scale-up of the PDMS based mechanical exfoliation process for high yield production of high quality graphite sheets of the desired thickness and with fewer number of defects.

CHAPTER 1. INTRODUCTION

1.1 Background

The class of two dimensional (2-D) van der Waals materials, which exist in bulk form as a stack of mono-layers with strong covalent bonding within each layer and weak van der Waals force between the layers, is of immense interest to researchers today due to their promising characteristics. The primary 2-D van der Waals material is graphene, a single atomic layer of graphite (Figure 1.1a) with its carbon atoms arranged in a 2-D honeycomb lattice, as shown in Figure 1.1b [1]. This material possesses remarkable mechanical, electronic, thermal, and optical properties. For example, graphene displays exceptional quantum hall effect [2], high electron mobility at room temperature of 2.5×10^5 $cm^2V^{-1}s^{-1}$, Young's modulus of 1 TPa, high thermal conductivity (> 3,000 WmK^{-1}), optical absorption of 2.3%, ability to conduct high densities of electric current, and chemical functionality [1, 3].

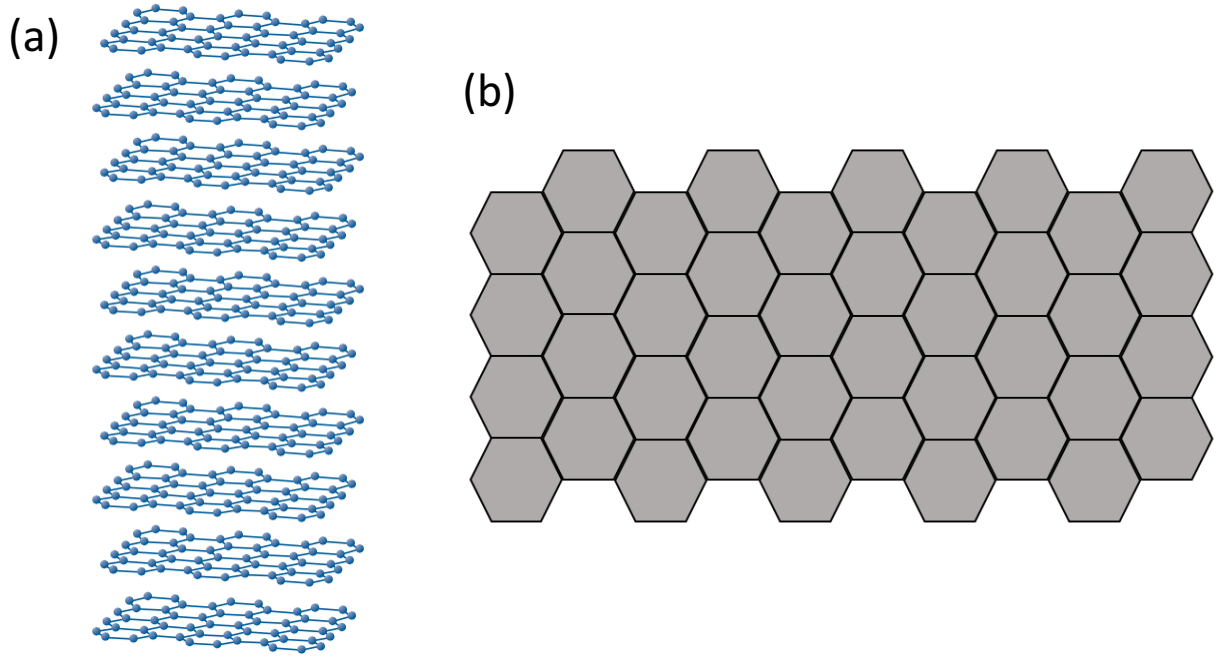

Figure 1.1: (a) Stacked 2D layer to form 3D graphite [1], and (b) 2D honeycomb lattice structure of graphene.

Graphene was first obtained by mechanical exfoliation through repeated peeling of graphite via adhesive tape (or scotch tape) [4]. An artificial form of high quality polycrystalline graphite called Highly Oriented Pyrolytic Graphite (HOPG), which has crystals oriented in the same direction, was used to mechanically exfoliate graphene. Prior to exfoliation, HOPG was plasma-etched to make 5 μm-deep mesas on its surface. The mesas were then brought into contact with spin coated photoresist and were separated after baking the photoresist. After separating the mesas from the HOPG, scotch tape was used to repeatedly peel off flakes of graphite mesas until thin flakes remained in the photoresist. The remaining thin flakes in the photoresist were then washed with acetone and then picked up by a 300 nm-thick SiO_2-on-Si wafer. Some of the thin flakes of graphite mesas were found to be mono- or few- layer graphene. These flakes of approximately 4

to several angstroms of thickness showed good agreement with the thickness of mono-or few-layer graphene, as shown in Figure 1.2.

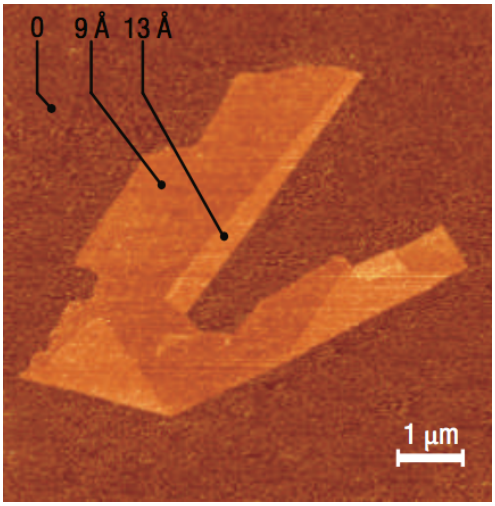

Figure 1.2: Graphene at different thicknesses by AFM [1].

Simpler ways of producing graphene by mechanical exfoliation avoid the use of photoresist. Prior research on mechanical exfoliation of graphene directly exfoliated graphite flakes by attaching the graphite flakes/scotch tape assembly on the SiO_2 substrate and obtained small size mono- or few- layer graphene [5].

Applications of graphene include transparent conductive coatings [3], paints [1, 6], graphene-based composite electrode [7], NEMS [8], and sensors [7, 8], as well as a number of photonic applications such as photodetectors, optical modulators, solid-state mode locked lasers, and optical polarization controllers [3]. More recently, graphene has emerged as a powerful, viable plasmonic material for fast electrical manipulation of light [9]. Potential applications of graphene as a plasmonic material include electro-optical modulation, optical sensing, quantum plasmonics, light harvesting, spectral photometry, and tunable lighting at the nanoscale [9].

Layers thicker than mono- or few-layer graphene, also known as pyrolytic graphite sheets (PGS), are often used as an effective heat transfer material. PGS of 0.1 mm thickness can be used as an effective cooling system in proton exchange membrane fuel cells (PEMFCs) because of its high thermal conductivity [10]. A 0.01 mm thick PGS is reported to have a thermal conductivity of 1950 W/m.K compared to a thermal conductivity of 700 W/m.K for a 0.1 mm thick PGS. Therefore, thinner multi-layer graphite sheets are more thermally efficient in transferring heat [11]. Even at a thickness of 500 μm, PGS is an efficient cooling/thermal interface for microprocessor chips [12]. PGS are also flexible and electrically conductive. Hence, the practical utility of 2D graphite layers extends from nanometer-scale thickness (mono- or few-layer graphene) to tens of micrometers in thickness (PGS).

1.2 Motivation and Problem Statement

A key requirement for practical application of 2D graphite layers of varying thickness is the capability to mass produce the layers in a controlled manner because the number of layers and defects in the layers significantly impact their thermal/electrical/optical transport properties. Methods such as mechanical and liquid-phase exfoliation, chemical vapor deposition (CVD), surface segregation, and molecular beam epitaxy (MBE) have been developed to create 2D layers of van der Waals materials [13, 14]. However, many of the useful applications require large-area, continuous 2D layers that are flat and have a high purity continuous structure with no mechanical and chemical imperfections. Cost-effective production of 2D van der Waals materials of varying thickness and minimal defects is an urgent challenge requiring further attention.

Among the existing graphene production methods, the mechanical exfoliation technique utilizing adhesive (scotch) tape is known to yield the highest quality graphene [3]. However, it is

mostly limited to use in research because of its low yield and inability to reliably produce large area 2D layers [15]. There is hence a need for developing a cost-effective, high yield, reliable manufacturing method for producing thin, large area (≥ square centimeters) 2D graphite layers of varying thicknesses suitable for a variety of applications. The current thesis seeks to fill this need through investigation of a viscoelastic polymer, namely polydimethylsiloxane (PDMS), stamp based mechanical exfoliation method to produce 2D graphite layers of varying thicknesses from a bulk graphite source.

1.3 Research Objectives

The primary research objectives of this thesis are:

1. To understand and quantify the effect of PDMS stamp curing time on the exfoliation process and on the layers exfoliated from the HOPG.
2. To understand and quantify the effect of surface roughness of the initial HOPG source on the exfoliated process.
3. To understand and quantify the effect of high frequency in-plane (shear) oscillation on the exfoliation process and on the resulting 2D graphite layers.
4. To understand and quantify the effect of PDMS stamp thickness on the exfoliation process and on the resulting 2D graphite layers.
5. To determine the combination of exfoliation process parameters that yield the thinnest 2D graphite layers.
6. To understand the scalability of the PDMS stamp assisted mechanical exfoliation process.

1.4 Approach

An experimental approach is used to achieve the abovementioned research objectives. PDMS is the primary adhesive polymer used to exfoliate the 2D layers from the bulk graphite source in this experiment. This approach is a variant of the well-established PDMS based transfer printing technique because it focuses on cleaving the industrially manufactured bulk 12 x 12 mm^2 HOPG and controlling the thickness of exfoliated layers by addressing the various process parameters, variables, and surface roughness. Curing time, adhesiveness, and lateral strain of PDMS stamp are considered to produce full areal (12 x 12 mm^2) exfoliation with as few surface defects as possible. External shear-based oscillation is also investigated to evaluate its effect on the exfoliation process and on thickness of exfoliated layers. These studies attempt to improve the PDMS stamp-assisted mechanical exfoliation process to repeatedly produce thin, large area graphite sheets of varying thicknesses and with minimal defects. Pertinent characterization methods, including confocal microscopy, contact or optical profilometry, micro-Raman spectroscopy, four-point probe method, and time domain thermoreflectance (TDTR) technique are used to characterize the properties of the exfoliated layers.

1.5 Thesis Outline

The rest of the thesis is organized as follows. Chapter 2 provides a comprehensive overview of prior research on mechanical exfoliation of graphene, other graphene production methods, deterministic assembly and transfer techniques using PDMS, and a new idea of applying external shear on the HOPG. Chapter 3 discusses about an experiment that exfoliated the bulk HOPG with PDMS stamps cured at different curing times and studied the effect of PDMS stamp curing time

on the exfoliated layers. Chapter 4 provides a discussion on an experiment that studied the effect of roughness of initial HOPG surface on the mechanical exfoliation process and on the exfoliated layers. Chapter 5 describes a new experimental approach to superpose shear oscillation/mechanism to the original normal exfoliation process and evaluates its effect on the thickness of exfoliated layers. Chapter 6 reports on exfoliating the HOPG with thin, uniform, spin-coated PDMS stamps to improve the quality of exfoliated layers. Chapter 7 describes an experiment that combined the two approaches used in Chapter 5 and Chapter 6, which were shearing the HOPG and exfoliating HOPG with thin, spin-coated PDMS stamps, respectively. Chapter 8 reports on a new set of experiments that created mesas or micro-pillars on the HOPG source and sought to study the scalability of the PDMS stamp based mechanical exfoliation process. Chapter 9 concludes this thesis with overall remarks and results that were reported in the previous chapters and provides future work to further improve the PDMS stamp based mechanical exfoliation of HOPG.

CHAPTER 2. LITERATURE REVIEW

Chapter 1 introduced graphene as the primary 2D van der Waals material, its potential applications, and its production via mechanical exfoliation of HOPG. Additionally, Chapter 1 explained the background, motivation, and research objectives of the thesis. This chapter presents a literature review of prior research pertinent to the research objectives. It also presents a thorough comparison of various graphene production/synthesis methods to motivate the development of a mechanical exfoliation technique to reliably produce large area (square centimeter size) 2D graphite layers of a wide range of thicknesses including mono- and multi-layer graphene. Prior research on PDMS as it relates to use in mechanical exfoliation and transfer printing processes is also reviewed.

2.1 Graphene Production Methods

The application of graphene and similar 2D materials largely depends on reliable and scalable production of high-quality large-area sheets while preserving its unique physical and mechanical properties [16]. These properties are strongly affected by the synthesis or production method [17]. Existing graphene production methods can be broadly classified into three groups: epitaxial growth, unconventional methods, and exfoliation techniques [18]. In epitaxial growth, graphene is grown on a substrate using chemical or physical vapor deposition (CVD or PVD) techniques. These chemically assisted methods are capable of producing large-area graphene layers. Attempts to scale up the CVD method using a roll-to-roll production process have been reported [3, 19, 20]. When grown on a nickel layer and subsequently transferred onto a substrate, graphene can be used as a stretchable transparent electrode [21]. However, CVD graphene layers

tend to have lower charge carrier mobility, a key factor for electronic applications, compared to mechanically exfoliated graphene [3]. CVD graphene layers also contain intrinsic holes, as shown in Figure 2.1 [22]. The class of unconventional methods includes techniques such as unzipping Carbon Nanotubes (CNTs), arc discharge, and detonation of chemicals [23-26]. These methods suffer from limitations that include poor yield, use of hazardous chemicals, contamination of graphene with impurities and functional groups, and long processing times. A relative quality and cost comparison of major mass-production methods for graphene is given in Figure 2.2.

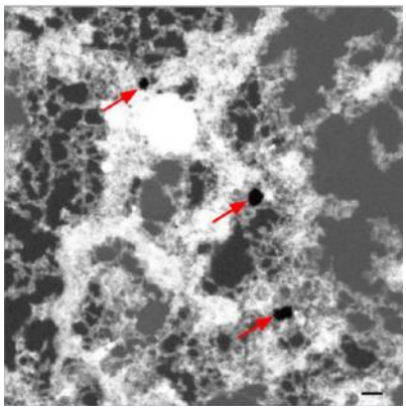

Figure 2.1: Intrinsic holes in CVD graphene by STEM (Scale bar is 10 nm) [22].

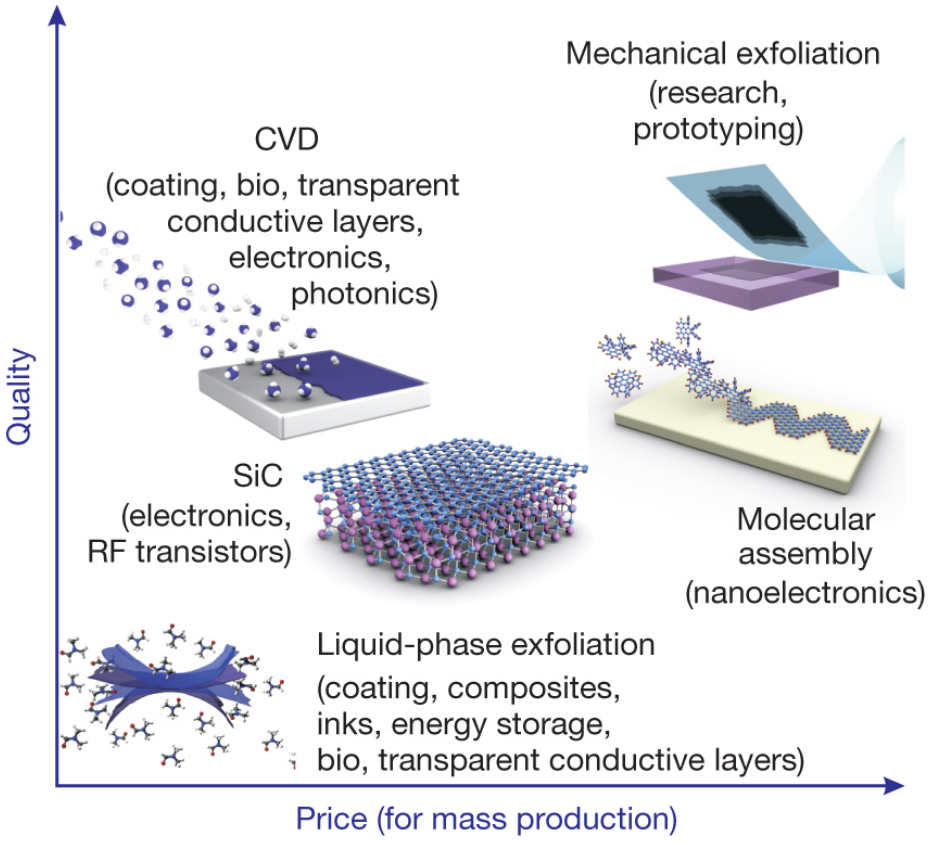

Figure 2.2: Major mass-production methods of graphene and their comparison [3].

The exfoliation process routes consist of chemical, thermal, and mechanical methods. In chemical and thermal exfoliation methods, colloidal suspension and intercalation techniques are used to produce mono- and few-layer graphene [11,24]. These techniques suffer from limitations of size of exfoliated layers, poor quality, contamination by various functional groups, and the use of hazardous chemicals [27]. The adhesive tape (or scotch tape) based mechanical exfoliation process is reported to be the best process for producing high quality graphene sheets, but it suffers from low yield and small size of sheets (~ ten to hundred microns square) [3]. It is mostly restricted to laboratory research. Comparing CVD graphene and mechanically exfoliated graphene via Raman spectroscopy in Figure 2.3, CVD graphene possesses a D peak at 1360 cm^{-1}, meaning

disordered structure or defect, but the mechanically exfoliated graphene does not exhibit this characteristic [28]. Defect-less graphene obtained by mechanical exfoliation is useful for practical applications provided the size and yield limitations of the exfoliation process can be overcome. Another mechanical exfoliation method that uses an atomic force microscope (AFM) tip to exfoliate graphite by scratching on Highly Ordered Pyrolytic Graphite (HOPG) mesas has been reported [29, 30]. Apart from this, a wedge based mechanical exfoliation technique was also investigated as an alternative mechanical exfoliation technique [31, 32]. There are several clear differences between chemical and mechanical exfoliation, as listed in Table 2.1.

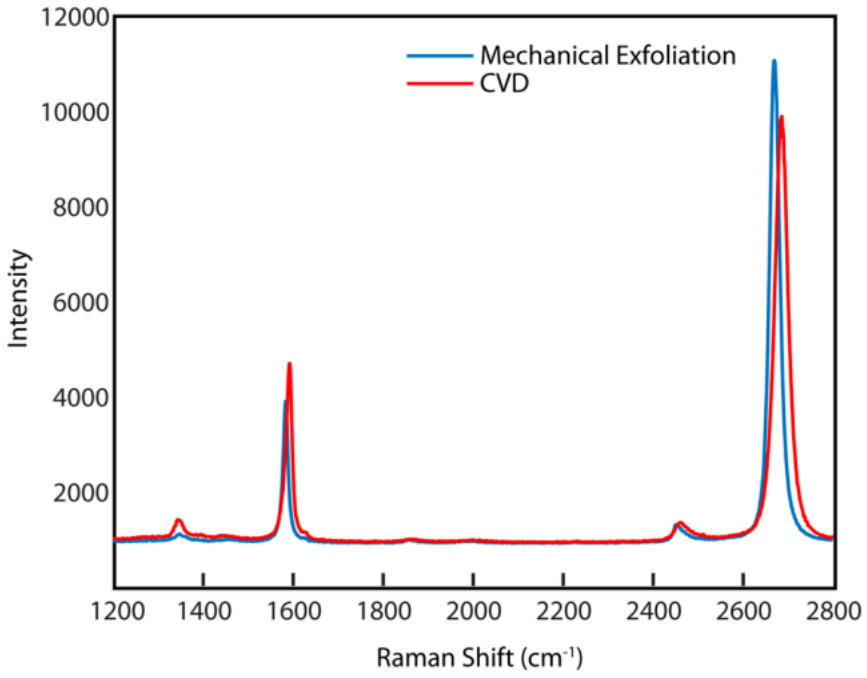

Figure 2.3: Raman spectra of mechanically exfoliated graphene and CVD graphene [28].

Table 2.1: Chemically grown versus mechanically exfoliated layers.

Characteristics	**Chemical**	**Mechanical**
Yield	CVD- High Colloidal- Low	Low
Size (Area)	CVD-Large (~50 mm^2) Colloidal-Medium	Medium (~100 μm^2)
Separation	Overlap	Easy
Carrier mobility	Low	High

None of the existing graphene production methods is considered to be a scalable and reliable fabrication technique for producing high quality, large area graphene/multi-layer graphite for practical applications. Although the CVD method is capable of producing large area mono- and few-layer graphene, its quality is not on par with mechanically exfoliated graphene, as already discussed. Hence, this is a nascent area for research into scalable and reliable production methods for large area, high quality graphene and multi-layer graphite production. There are several challenges to be addressed in developing a new fabrication technique for this novel material such as preserving sheet thickness uniformity, producing them at lower cost than existing methods, ensuring high yield at faster production rates, ensuring scalability to high volumes, and producing it in a pure state without defects.

2.2 PDMS-based Transfer Printing and Exfoliation Methods

This thesis uses polydimethylsiloxane (PDMS) stamp to mechanically exfoliate 2D graphite sheets of varying thicknesses from HOPG. PDMS is a common silicon-based viscoelastic polymer used for “transfer printing” of micro- or nano-scale objects from one substrate to another. As shown in Figure 2.4, this technique can be used for additive transfer, subtractive transfer, and

deterministic assembly of micro- or nano-structured objects including semiconductor materials [33-35]. PDMS-based stamping processes do not require conventional adhesives or hazardous chemicals. The process takes advantage of the rate or velocity dependence of the adhesion properties of PDMS. Printing can be effectively performed by varying the velocity of the PDMS stamping process to pick up or print various sizes of objects to realize heterogeneous integration or deterministic assembly; using a high rate lifting/peeling action picks up objects from the donor substrate while stamping at a low speed permits the object adhered to the PDMS stamp to be successfully transferred to the receiving substrate [36]. Using the kinetic control of adhesion to perform transfer printing, 3 to 12 nm thick graphene sheets were successfully transferred by a PDMS stamp onto a SiO_2 wafer, as shown in Figure 2.5. This polymer-based lithography process is useful for many applications including micro sensors, micro-electromechanical systems (MEMS), and micro-optical systems [37]. This simple, productive, and cost advantageous technique with the PDMS stamp has also been used to exfoliate graphene layers, as discussed below.

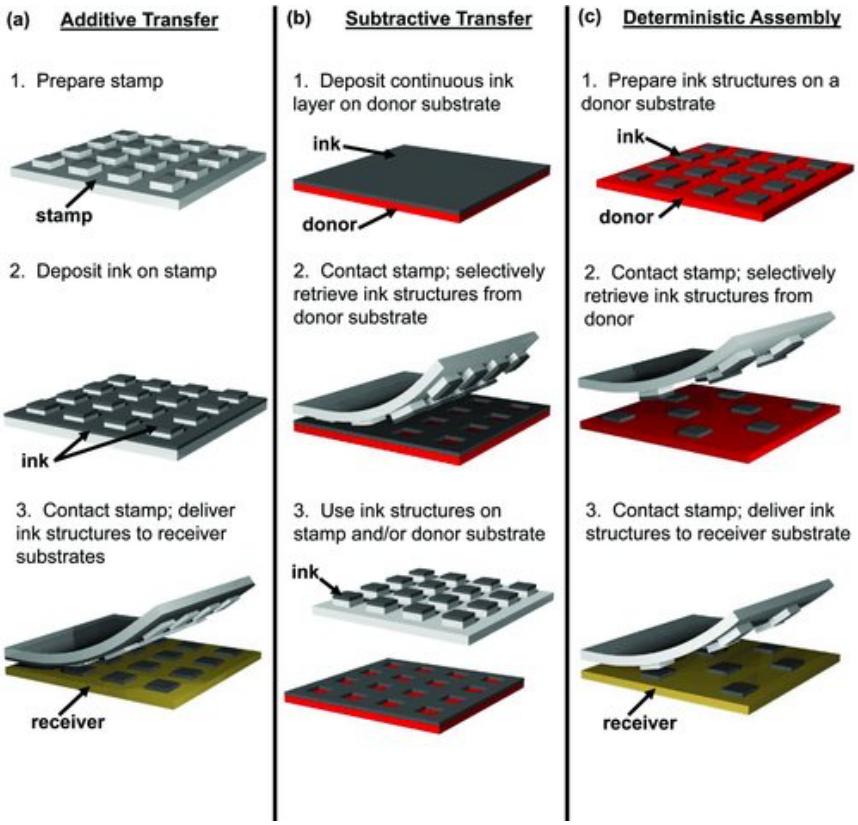

Figure 2.4: Three main uses of transfer printing [33].

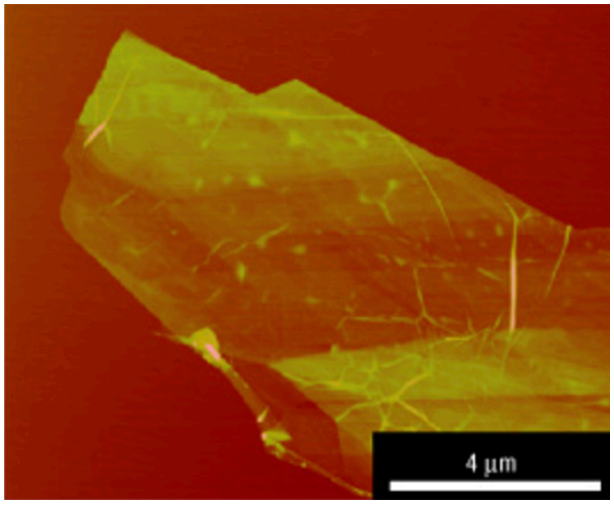

Figure 2.5: Transferred few-layer graphene on SiO_2 surface via transfer printing [36].

Some experiments with PDMS to mechanically exfoliate graphene have been reported. In one study, an experiment was conducted to directly exfoliate CVD graphite grown on a nickel foil using a PDMS substrate [38]. As shown in Figure 2.6, mono- and bi-layer graphene were exfoliated from a 400 x 400 μm^2 of 271 nm thick graphite grown on nickel foil. This graphene on PDMS substrate could potentially be used as a wafer-scale transparent, flexible, and stretchable electronics without having to transfer the graphene to a SiO_2 substrate [39]. The graphene on PDMS substrate is shown in Figure 2.7. However, this process involves CVD graphene, which is inferior to mechanically exfoliated graphene in terms of cost and quality. In addition, there is lack of knowledge of the systematic exfoliation parameters (e.g., exfoliation speed) required to successfully exfoliate graphene and the repeatability or yield of the process. Chemically transformed graphene obtained from graphite oxide in solution was also mechanically exfoliated using a PDMS stamp [40], but the size of the transferred graphene is small and inconsistent, and detailed knowledge of controllability and reliability of the process is lacking. More significantly, these techniques with PDMS stamps have not been used to control the thickness of the exfoliated graphite layers to produce high quality graphene or thin graphite sheets for relevant applications.

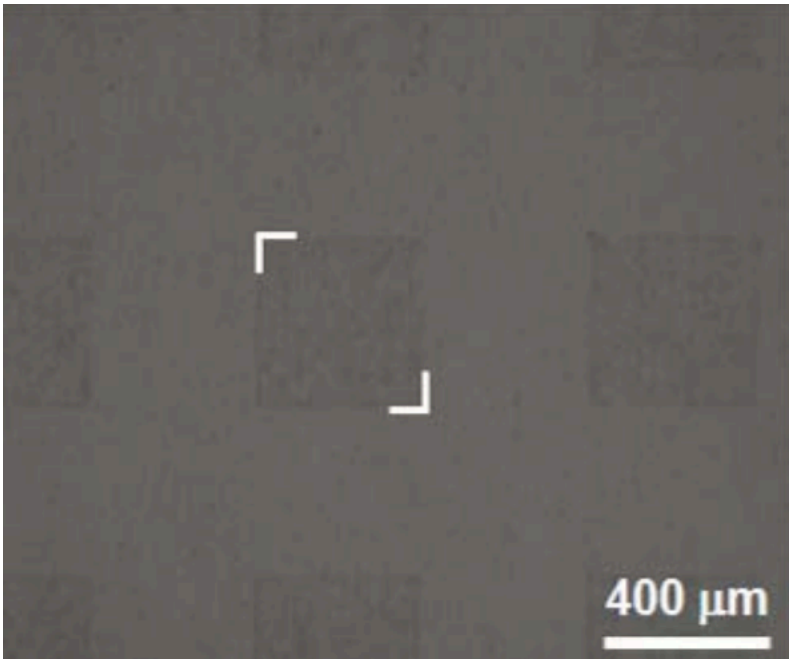

Figure 2.6: Few-layer graphene on PDMS [38].

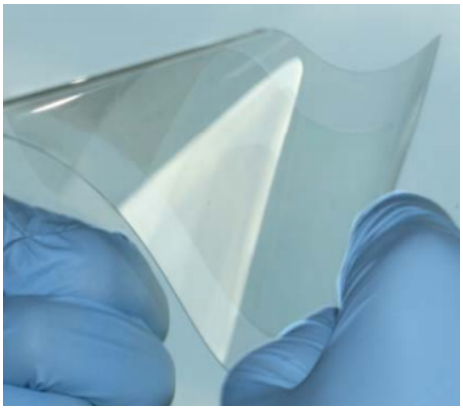
Figure 2.7: Graphene on transparent, flexible, and stretchable PDMS substrate [39].

There is evidence of strong van der Walls and/or capillary forces responsible for adhesion between graphene flakes and a SiO_2 surface [1, 4]. Micro-pillars, or periodic arrays of patterns, can be easily created on HOPG via oxygen plasma etching [41]. Using this approach, HOPG was etched to create patterned 6 x 6 x 8 μm^3 mesas on its surface, as shown in Figure 2.8. The mesas were directly stamped onto a SiO_2 substrate to exfoliate few-layer graphene [42]. This process

does not involve any interfacial medium to exfoliate or transfer to the receiving substrate, and it is able to produce few-layer graphene with a thickness of 3.6 nm, as shown in Figure 2.9. However, the researchers responsible for this work acknowledge that uniform large area exfoliation of few-layer graphene needs improved stamp-preparation and exfoliation practice as the thickness of the transferred layer is not consistent. Furthermore, their study lacks information concerning the process parameters and variables used to stamp few-layer graphene. Despite the promising results, the size (surface area) of the few-layer graphene obtained using this method is small. This process was later improved by embedding the mesas in PDMS and then using the mesas-PDMS assembly to stamp patterned graphene onto a silicon wafer [43]. This process allows more uniform stamping but lacks details of the stamping parameters, and it is limited to small micro-pillars. A similar experiment was performed with laser-scribed square patterns on HOPG to exfoliate mono- or few-layer graphene on an oxidized silicon wafer [44]. However, the yield of this process is low and the size of the layers is much smaller than the size of the initially scribed patterns. Another experiment was conducted without etching any patterns on graphite but by directly stamping bulk graphite using a PDMS stamp, followed by exfoliation with a secondary PDMS stamp [45]. This work, including other work discussed earlier, has the capability of producing mono- or few-layer graphene, but again the layer size and process controllability are the main issues. From an application standpoint, the exfoliation process needs to be more controllable and repeatable in consistently producing large area mono- and few-layer graphene.

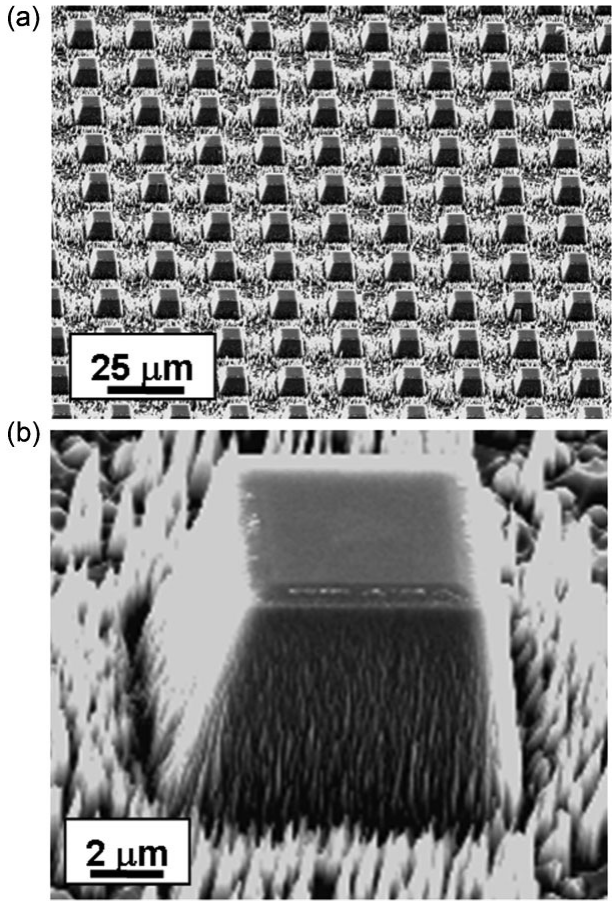

Figure 2.8: Mesas on HOPG at (a) low magnification and (b) high magnification [42].

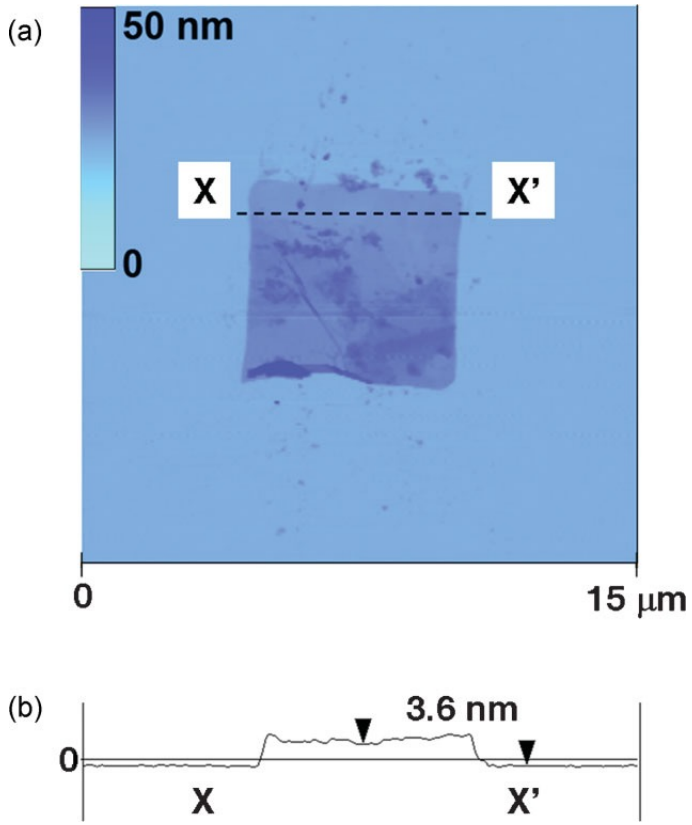

Figure 2.9: (a) Few-layer graphene on substrate (b) AFM profile of the layer [42].

2.3 Summary

The motivation for the development of a cost-effective, high yield, reliable production method for mechanically exfoliating large area (square centimeter size) 2D graphite layers of varying thicknesses, including mono- and few-layer graphene, originated from a thorough literature review of various methods including PDMS stamp based transfer printing and PDMS-assisted exfoliation of mono- or few-layer graphene. It is evident from the literature review that there does not exist a reliable mechanical exfoliation method capable of producing high quality square-centimeter-size large area 2D graphite sheets of varying thicknesses directly from HOPG. In particular, detailed knowledge of the influence of various exfoliation process parameters on the exfoliation process and on the resulting exfoliated layer quality is not available. Therefore, this

thesis focuses on addressing these limitations of the PDMS-stamp based mechanical exfoliation process. Specifically, it experimentally investigates the effect of various exfoliation process parameters including PDMS stamp properties such as stiffness, and process variables such as exfoliation speed, normal contact force, and dwell time, and the influence of the initial surface condition of the HOPG source material on the exfoliated layer characteristics such as surface morphology, defect structures, roughness, and certain physical properties such as thermal conductivity and electrical sheet resistance. A novel aspect of this thesis is the investigation of the effect of high frequency shear oscillation to control 2D layer thickness. This idea stems from the recognition that the van der Waals bonds between the 2D layers of graphite can be mechanically broken using either a normal force or a shear force or their combination [46].

The following chapters report on the experimental work aimed at addressing the above aspects pertaining to the stated research objectives of the thesis.

CHAPTER 3. EFFECT OF PDMS STAMP CURING TIME ON MECHANICAL EXFOLIATION OF HOPG

3.1 Introduction

Preliminary work on mechanical exfoliation of HOPG using a PDMS stamp showed that it is possible to produce multi-layer pyrolytic graphite sheets with fairly large surface area (on the order of square centimeters) [47]. However, the surfaces of the exfoliated sheets obtained were characterized by large flat patches, compressed regions, wrinkles, torn edges, and folds. It is therefore crucial to understand how to control such defect structures in order to produce higher quality exfoliated surfaces. One reason for such defects is stretching of the exfoliated layers due to the polymer's elasticity during initial contact with the HOPG surface followed by relaxation of the strains during exfoliation. Consequently, the effect of PDMS stiffness, which is controlled by varying the curing time, on the exfoliation process needs to be evaluated. This chapter discusses an experiment on mechanical exfoliation using PDMS stamps of different stiffness. It also describes the specific process parameters and conditions used to exfoliate graphite layers from the HOPG.

3.2 Experimental Setup and Procedure

This section describes the general experimental setup and procedure used for the PDMS-assisted mechanical exfoliation of large area thin graphite layers, along with the experiments designed to study the effect of different curing times of the PDMS stamp on its stiffness and on subsequent exfoliation. It elaborates on the experimental procedure mentioned briefly in Chapter 1. The main apparatus and methods for the exfoliation process remain unchanged from the experimental setup used in the preliminary investigation reported earlier [47]. Each experiment in

this thesis incorporated the same procedures for preparing the PDMS stamp and for the exfoliation tests. Modifications made to this apparatus to test the effect of different process variables, surface roughness, and high frequency shear oscillation will be explained in the following chapters.

Figure 3.1a shows a schematic of the basic apparatus used for exfoliation. The exfoliation procedure is shown schematically in Figure 3.1b. The apparatus permits a controlled study of the exfoliation process parameters, which include the normal force, dwell time, and exfoliation speed. A three-axis piezoelectric force dynamometer (Kistler 9256) placed underneath the HOPG sample (SPI-ZYA at a size of 12 x 12 mm^2) was used to measure the instantaneous exfoliation forces in three orthogonal directions including the direction of exfoliation. The HOPG sample was fixed to the dynamometer via double-sided scotch tape. The PDMS stamp was attached to a glass slide and glued to the stamp holder. The HOPG sample was then brought into contact with the PDMS stamp. After the desired normal contact force was reached, contact between the HOPG and the PDMS stamp was maintained for a short period (dwell time). Subsequently, the HOPG was retracted from the stamp at a specified exfoliation speed resulting in separation of a certain thickness of graphite from the bulk HOPG. Before and after each run, the HOPG sample was cleaned using manual exfoliation via scotch tape. The above procedure was used to study the stated research objectives of understanding the effects of process variables on the exfoliation process and on the size and quality of the exfoliated layers. In this chapter, PDMS stamps were cured at different curing times to understand the effect of stamp stiffness on the exfoliation process and on the layers exfoliated from the HOPG.

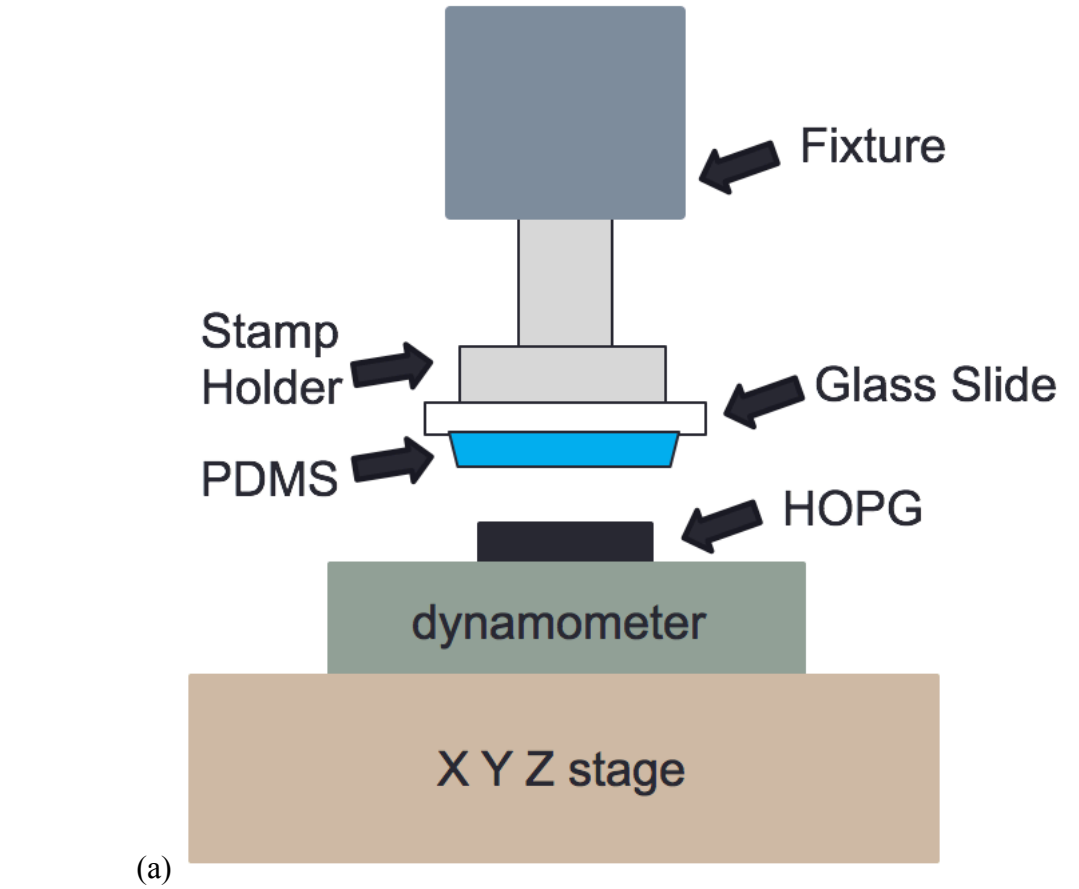

(a)

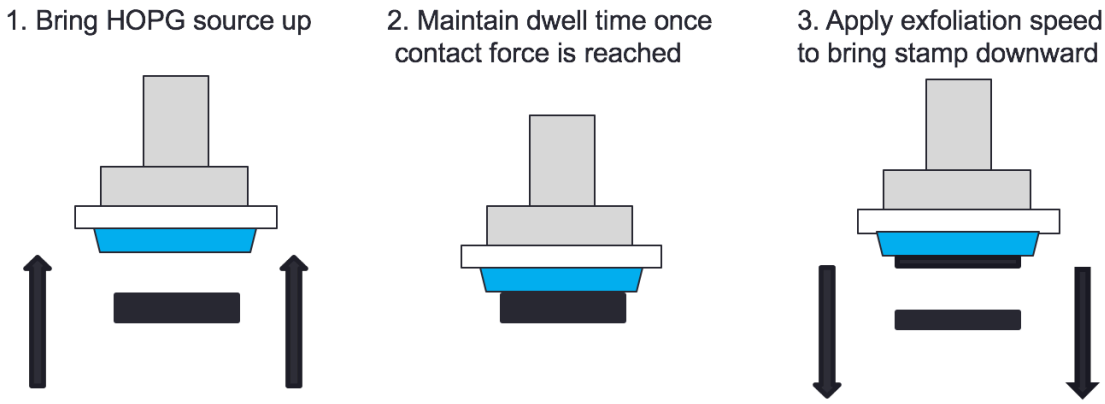

(b)

Figure 3.1: Schematic diagram of (a) experimental test-bed, and (b) exfoliation procedure.

PDMS stamps were prepared using a Sylgard 184 monomer-curing agent kit. Initially, a mixing ratio (by weight) of 10:1 of base and curing agent, respectively, was used. The monomer-curing agent mixture was then stirred for a few minutes and degassed in a vacuum desiccator for 20 minutes under -0.8 KPa pressure. The mixture was then poured into a 50 x 50 x 6.25 mm^3 glass container and cured for different time durations (depending on the purpose of each experiment) in a furnace at 70 °C. After completion of the cure cycle, the sample was transferred to a freezer for 1 hour to arrest the rapid thermal softening normally observed after furnace curing. A 15 x 15 mm^2 PDMS stamp, cut from each cured sample, was then used for each exfoliation trial. The thickness of the PDMS stamp was about 3 mm once it is completely prepared. Using the PDMS preparation method described above, the effect of PDMS stamp curing time was studied to find the optimum curing time (or stiffness) of PDMS that can repeatedly produce thin graphene/graphite sheets with minimum number of defects.

The stiffness of PDMS can be controlled by changing its Young's modulus, which can be tailored by varying the furnace curing time during stamp preparation. Hence, a set of experiments was planned and conducted to find the effect of different Young's modulii of the PDMS on the exfoliation characteristics. PDMS stamps were prepared in the same manner as discussed above. However, different furnace curing times of 25, 40, 60, 80, and 100 minutes were used to prepare the stamps. Greater curing times produced stiffer and less adhesive stamps. Exfoliation experiments were then conducted by fixing the normal contact force at 10 N, dwell time at 5 minutes, and the exfoliation speed at 30 mm/s. These process parameters, or exfoliation conditions, were obtained from a preliminary design of experiments (DOE). A normal contact force of 10 N, dwell time of 5 minutes, and exfoliation speed of 30 mm/s were chosen because these conditions

exfoliated the largest surface area of layers from the HOPG, as shown in Table A.1. Under these exfoliation conditions, three replicates were performed for each run.

After each run, the exfoliated graphite layers were characterized. Optical microscopy (Zygo NewView 200) and confocal microscopy (Olympus LEXT) were used to qualitatively evaluate the morphology of exfoliated layers and to measure the thickness of their edges, respectively. As explained in prior work and shown in Figure 3.2 [47], multiple thickness measurements of the exfoliated sheet edges were made and then averaged to obtain the estimated thickness of the exfoliated layers. These results showed that different PDMS stamp curing times have an effect on the exfoliation process and on the exfoliated layers.

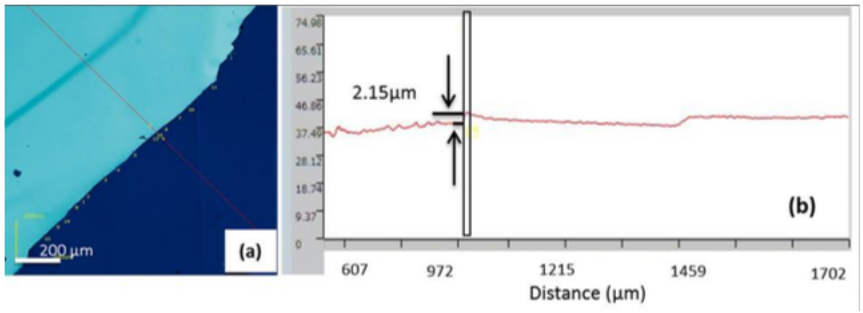

Figure 3.2: Thickness measurement technique of exfoliated layer showing (a) measurements performed along the edge, and (b) cross-sectional view of one profile [47].

3.3 Results and Discussions

Figure 3.3 shows the representative surface morphologies of the exfoliated layers obtained with the PDMS stamps produced under different curing conditions. It clearly shows fewer defect structures are present in the sheets exfoliated using the 60 min. cured PDMS stamp. The exfoliated sheets obtained with the 60 min. cured PDMS stamp have visibly smoother surfaces than the other

cases. This curing condition also produced the most repeatable exfoliation results (not shown in the figure). The exfoliated sheets produced by the 25 and 40 min. cured PDMS stamps show more defect structures. These sheets contain noticeable tattered edges, incomplete corners, uneven surface with larger wrinkles and cracks. The 25 and 40 min. cured PDMS stamps were less rigid and more adhesive than the 60 min. cured stamp. These results suggest that the higher elasticity (and therefore lower stiffness) of the 25 and 40 min. cured stamps causes greater transverse elastic deformation of the stamp during application of the normal force in the exfoliation process. This elastic deformation recovers during retraction of the stamp during exfoliation and causes in-plane compression of the exfoliated layer. The stamps cured for longer than 60 min. were more rigid and the exfoliated layers obtained using these stamps show more defect structures (see Figure 3.3d & e). While the more rigid PDMS stamps, which were cured for 80 and 100 minutes, had less elastic deformation, they also were less adhesive. Consequently, only partial exfoliations along with other defect structures were obtained using these stamps. Large wrinkles were present in the exfoliated sheets and portions of them were peeled-off or cracked. These results indicate that the PDMS stamp cured for 60 min. at 70^0C yields the optimum stamp properties for exfoliation. The surface areas of the exfoliated layers obtained with the 60 min. cured PDMS stamp were approximately 12 x 12 mm^2 (same as the initial size of the HOPG) and they had the least number of surface defects. The average thickness of one exfoliated sheet was found to be 62.3 ± 13.3 μm. The sheet thickness, as discussed previously, was determined by measuring the profile heights along the sheet edges in a confocal microscope.

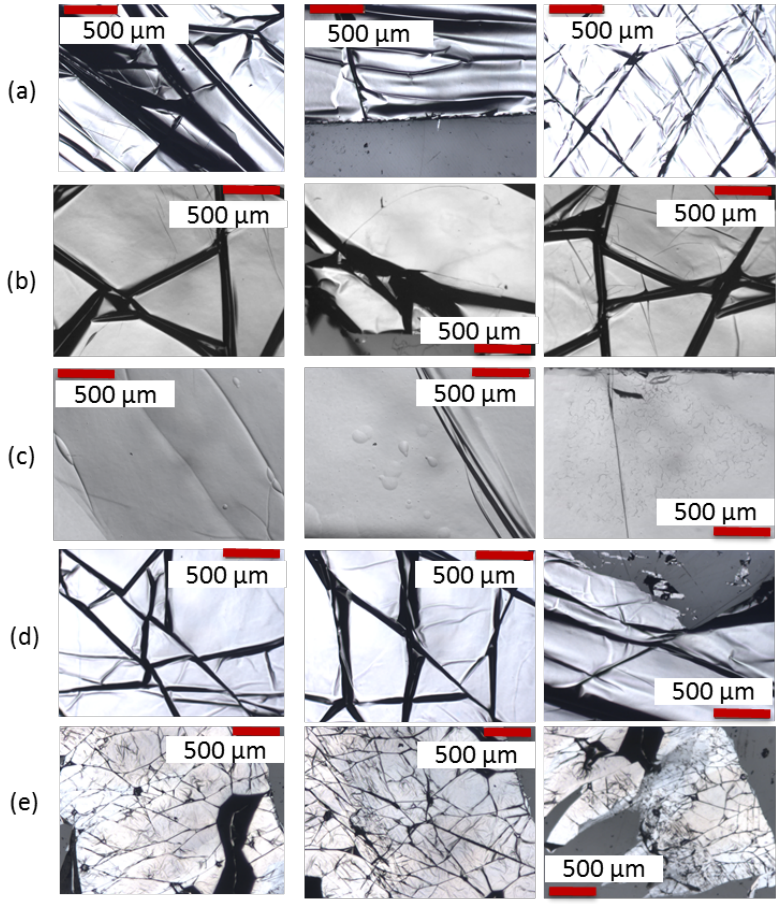

Figure 3.3: Exfoliated layers obtained with PDMS stamps cured for: (a) 25 min. , (b) 40 min., (c) 60 min., (d) 80 min., and (e) 100 min..

3.4 Summary

In this chapter, the basic experimental apparatus, the mechanical exfoliation procedure, and experiments aimed at understanding the effect of curing time of the PDMS stamp on the mechanical exfoliation process were discussed. Specifically, five different curing stamp times were used to prepare PDMS stamps of different stiffness and their effects on the exfoliation process and on the layers exfoliated from the HOPG were analyzed. The results showed that the 60 min. cured PDMS stamp yielded large area (12 x 12 mm^2) 62.3 ± 13.3 μm thick graphite sheets with the least number of surface defect structures. The following chapters discuss other experiments conducted to further reduce the number of defects and thickness of the exfoliated layers, and to produce consistent exfoliations at high yield.

CHAPTER 4. EFFECT OF ROUGHNESS ON MECHANICAL EXFOLIATION OF HOPG

4.1 Introduction

This chapter presents the results of experiments designed to investigate the effect of surface roughness of the HOPG source material on the exfoliation characteristics. The motivation for this experiment comes from a number of preliminary experiments that revealed a dependence of the size and quality of the exfoliated layers on the roughness of the initial HOPG surface. Additionally, the chapter also addresses the effect of surface roughness of the exfoliated graphite sheet on the ability to manually transfer print it onto a Si/SiO_2 wafer for further characterization or processing [48, 49] . Prior work on transfer printing of silicon structures onto a Si substrate via a PDMS stamp has shown that the presence of asperities on the surface can inhibit the transfer printing process [36].

4.2 Experimental Procedure

The main objectives of the experiments discussed in this chapter were to vary the roughness of the HOPG surface, track the HOPG surface roughness in each step of the exfoliation process, and to identify the exfoliation process parameters that permit complete exfoliation of sheets with the least number of defects. An additional objective was to understand the effect of surface roughness of the exfoliated sheets on the ability to transfer print them onto a Si/SiO_2 wafer for ease of further characterization and processing, including device fabrication.

The first step involved preparing HOPG samples with two distinct surface roughnesses prior to performing PDMS stamp-assisted mechanical exfoliation experiments on each of them. The two different surface roughnesses were obtained through careful manual cleaning of the HOPG using scotch tape based cleaving. One HOPG sample was denoted “smooth” because it was

cleaned via multiple swipes of the scotch tape that removed all visible, protruding flakes on its surface, while the second HOPG sample was denoted "rough" because it was cleaned using only one swipe of the scotch tape. The two levels of surface roughness thus obtained are clearly distinguishable, as shown in Figure 4.1. Also, the average areal arithmetic surface roughness values of the two cleaned HOPG surfaces were obtained by averaging ten random optical surface profilometer based measurements made on each of the two HOPG samples. The two HOPG surfaces were then subjected to the PDMS stamp-assisted mechanical exfoliation process, which was described in the previous chapter.

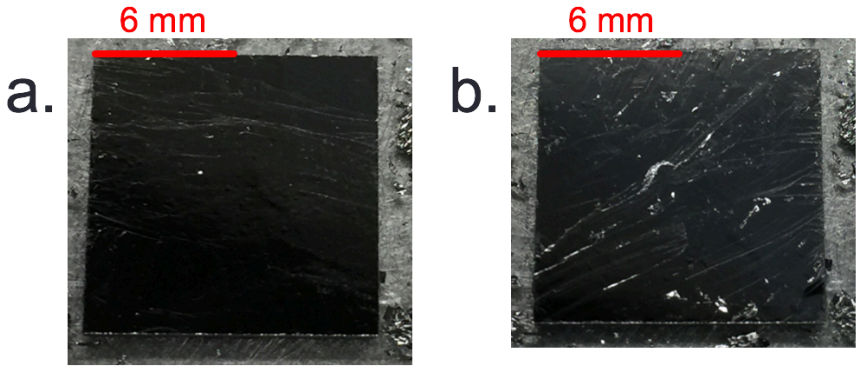

Figure 4.1: HOPG with (a) "smooth" surface, and (b) "rough" surface prepared by scotch tape based cleaving.

The PDMS stamps used in the exfoliation experiments were prepared using the optimal curing time of 60 min. and curing temperature of 70^0C established in the previous chapter. A normal contact force of 10 N, dwell time of 5 minutes, and an exfoliation speed of 35 mm/s were used to exfoliate the graphite sheets from the two HOPG surfaces. Note that a slightly higher exfoliation speed (35 mm/s) than established in the previous chapter (30 mm/s) was used in these experiments because the faster speed tended to yield more repeatable results. Two replicates of the

exfoliation experiment were performed for each surface roughness case. The size (surface area) and surface defects present in the exfoliated sheets obtained were analyzed using an optical microscope and the results are presented and discussed in the following section.

In addition to analyzing the effect of surface roughness on the exfoliated layer characteristics, additional experiments were performed with the "smooth" HOPG sample to track the surface roughness in every step of the exfoliation and transfer printing processes. The "smooth" HOPG surface was chosen because, as shown in the next section, the exfoliated graphite layers obtained from the "rough" HOPG sample had too many defects and tended to have smaller surface area. The exfoliation process conditions used in the tracking experiment were identical to those used in the first experiment described above. The only additional step beyond PDMS stamp based exfoliation consisted of transfer printing the exfoliated graphite layers onto a 100 mm diameter Si/SiO_2 wafer using a manual transfer printing process established during the course of this research. A schematic of the manual transfer printing process used is shown in Figure 4.2.

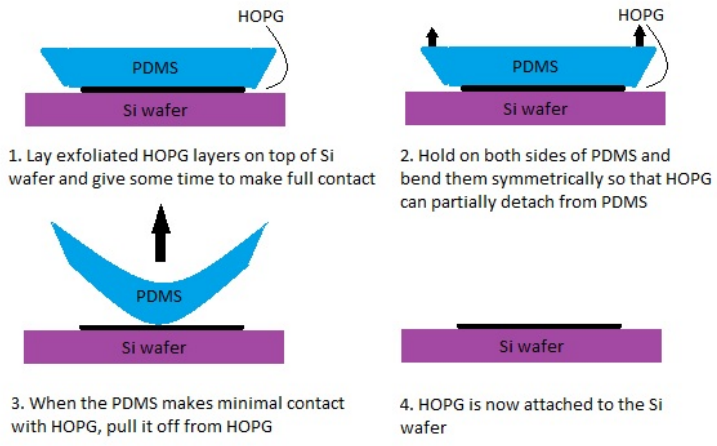

Figure 4.2: Manual transfer printing process used to transfer the exfoliated graphite sheet onto a 100mm (4 inch.) Si/SiO_2 wafer substrate.

4.3 Results and Discussion

The average areal arithmetic surface roughness (S_a) values for the two replicates of the "smooth" HOPG samples were 0.24 ± 0.14 μm and 0.24 ± 0.09 μm, respectively (only one representative surface is shown in Figure 4.1a). The corresponding average surface roughness values of the two "rough" HOPG samples were 0.99 ± 0.94 μm and 0.84 ± 0.63 μm, respectively. Figure 4.3 shows three representative surface morphologies of the exfoliated layers obtained from two surface roughness cases. The exfoliated layers obtained from the "smooth" HOPG surface contain fewer defects and have mostly full areal coverage of 12 x 12 mm^2 (not shown in the figure.) The exfoliated layers obtained from the "rough" HOPG surface contain more defects including large wrinkles, and they are smaller in size than the layers obtained from the "smooth" HOPG surface. These results illustrate that the initial roughness of the HOPG surface prior to exfoliation plays a critical role in determining the quality of the exfoliated layers. As seen, a clean and smooth HOPG surface yields exfoliated graphite layers that are larger in size and have fewer defects. The replication tests showed that the "smooth" HOPG samples yielded more consistent results than the "rough" HOPG samples.

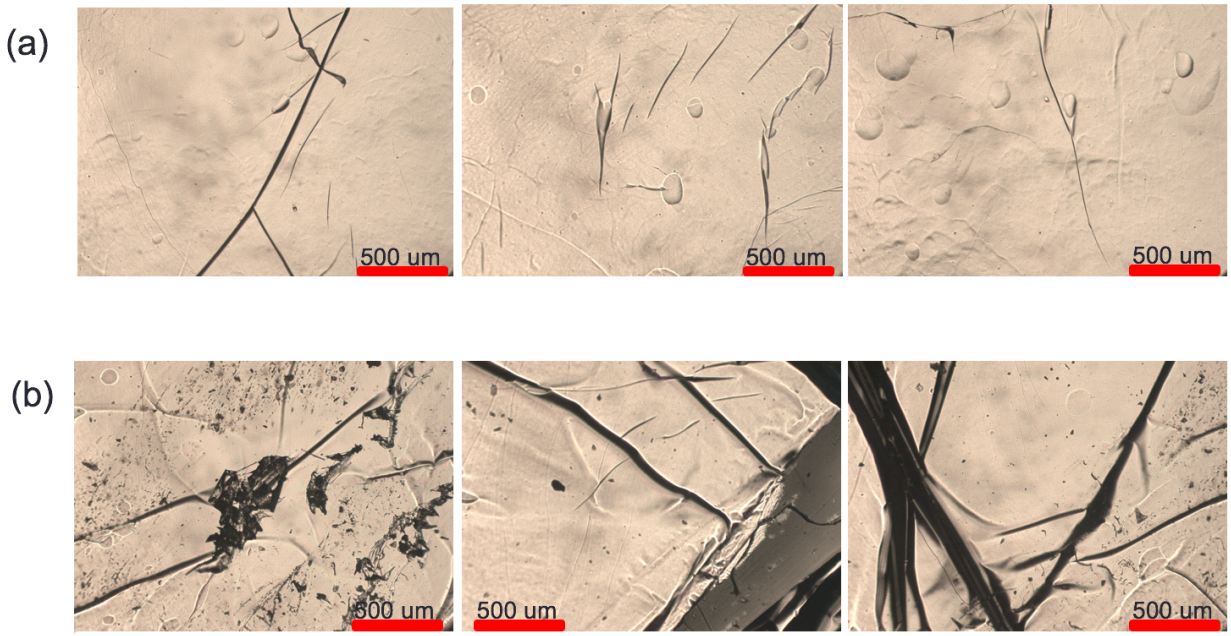

Figure 4.3: Exfoliated layers obtained from (a) "smooth" HOPG surface, and from (b) "rough" HOPG surface.

The results of the surface roughness tracking experiment using the "smooth" HOPG sample is shown in Figure 4.4. In this experiment, the average areal arithmetic surface roughness of the "smooth" HOPG sample was 0.21 ± 0.17 µm (Figure 4.4a). The average surface roughness of the exposed surface of the exfoliated layer (when still attached to the PDMS stamp) was 0.18 ± 0.09 µm. The exfoliated layer was subsequently transferred to a very smooth ($S_a \sim 3$nm) Si/SiO_2 wafer (Figure 4.4c). The average roughness of the exposed surface of the transferred layer (previously attached to the underside of the PDMS stamp) was 0.38 ± 0.33 µm, which is higher than the roughness of the original exfoliated surface prior to transfer printing. This indicates that the transfer printing process introduces additional roughness most likely due to the deformation of the sheet during the transfer printing process. It should also be noted that manual transfer was not successful in some cases as the graphite sheets contained visible asperities, which hindered

adhesion of the sheet to the wafer; in such cases, the exfoliated layer remained attached to the PMDS stamp instead of being transferred to the wafer surface. As noted earlier, the exfoliated sheet obtained from the "rough" HOPG sample was difficult to transfer to the Si/SiO_2 wafer because the sheet was incomplete and had more defects. These results confirm that the exfoliation process and the transfer printing process are sensitive to the initial surface condition of the HOPG. In general, exfoliated sheets with lower roughness were obtained when the initial HOPG surface roughness was less than 0.24 µm.

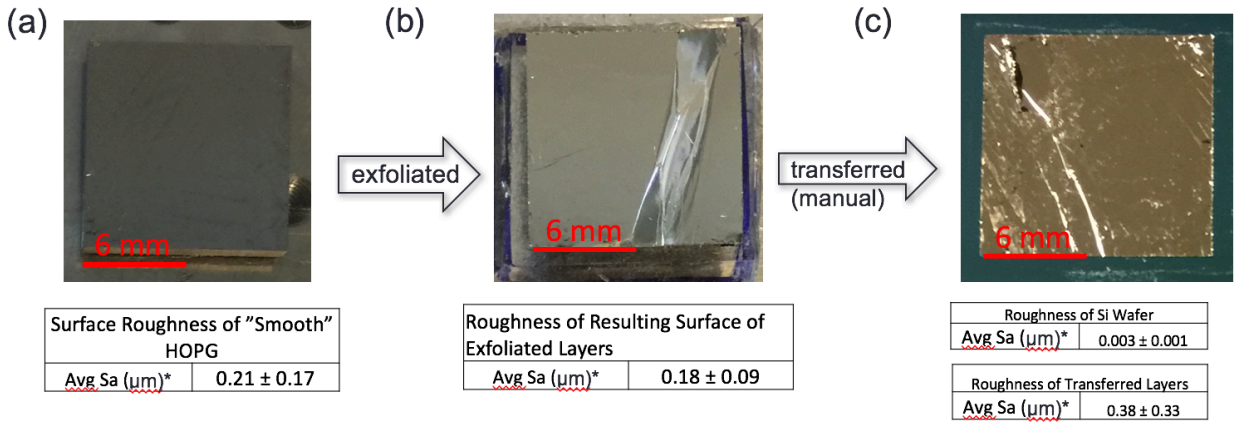

Figure 4.4: (a) "Smooth" HOPG surface prior to exfoliation, (b) Morphology of exposed surface of sheet after exfoliation, (c) Morphology of exfoliated sheet after transfer onto silicon wafer.

4.4 Summary

This chapter investigated the effect of surface roughness of the initial HOPG source on the exfoliated layers/sheets. The results showed that the PDMS stamp based mechanical exfoliation process of HOPG is sensitive to the initial surface condition of the HOPG. Full area exfoliations with low surface roughness were obtained when the initial HOPG average arithmetic surface roughness was less than 0.24 μm. In addition, the exfoliated layer could also be successfully transferred onto a Si/SiO_2 wafer. The results of the experiments in this chapter also showed that the transfer printing process introduces additional surface roughening, potentially due to the deformation of the exfoliated sheet during the transfer printing process. The findings of this chapter informed the preparation of the HOPG samples in the experiments reported in the following chapters.

CHAPTER 5. EFFECT OF HIGH FREQUENCY SHEAR OSCILLATIONS ON MECHANICAL EXFOLIATION OF HOPG

5.1 Introduction

In this chapter, the effect of high frequency shear oscillation on the thickness of exfoliated sheets is investigated with the goal of producing thinner layers of pyrolytic graphite sheets, and eventually mono- or few-layer graphene. The hypothesis is that introducing a low amplitude shear-type oscillation in the plane of the graphite layers will promote cleavage close to the PDMS stamp-HOPG interface, thereby yielding thinner sheets. As discussed earlier, this idea originated from the recognition that the bonds between the 2D layers of graphite can be mechanically broken using either a normal force or a shear force or their combination [46].

5.2 Experimental Procedure

Superposition of the high frequency shear oscillation on the standard PDMS stamp based mechanical exfoliation process described earlier required the installation of a piezoelectric shear actuator (Polytec PI, Model P-112.03) into the experimental setup used in the exfoliation experiments reported in the previous chapters. Figure 5.1 shows a schematic of the exfoliation process in the presence of shear oscillation caused by a piezoelectric shear actuator placed underneath the HOPG sample. The amplitude of shear excitation was ±1 μm about the equilibrium position and is a function of the voltage applied to the actuator. The total shear displacement of 2 μm was verified by observing the displacement of the shear actuator in an optical microscope by applying input voltages of -75 and +75 V. The limited surface area of the shear actuator (3 x 3 mm^2) restricted the initial surface area of the HOPG to approximately 6 x 6 mm^2 to permit a stable

exfoliation process. To do so, the original HOPG sample (12 x 12 mm^2) was sectioned with a razor blade.

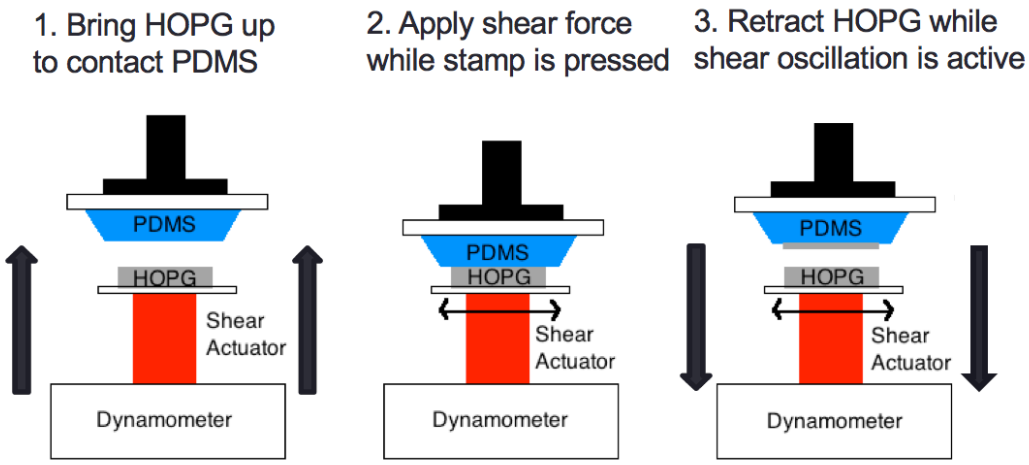

Figure 5.1: Exfoliation process in the presence of shear oscillation.

The PDMS stamps used in this experiment were prepared in the same way as in the previous experiments up to the point they were poured and cured in the 50 x 50 x 6.25 mm^3 glass container. Since the size of the HOPG was reduced to 6 x 6 mm^2, the PDMS stamps were also cut to a smaller size of approximately 7 x 7 mm^2, instead of the original size of 15 x 15 mm^2. The thickness of the PDMS stamps (3 mm) remained the same as in prior experiments.

The mechanical exfoliation experiments in the presence of high frequency shear oscillation were performed using the procedure illustrated in Figure 5.1. The shearing frequency was varied from 500 to 3000 Hz in 500 Hz increments. Three replicates were performed for each test condition. The exfoliation speed and dwell time were fixed at 35 mm/s and 5 min., respectively. A normal contact force of 5 N was used in all experiments. The experimental procedure was as follows. The HOPG was brought into contact with the PDMS stamp and the specified normal force was applied (Figure 5.1a). After the desired normal force was reached, shear oscillation at a given frequency was applied (Figure 5.1b). Upon completion of the dwell time, the HOPG was retracted at the

exfoliation speed (Figure 5.1c). Of the three replicates for each shearing frequency value, the exfoliated layers/sheets with full areal coverage and of the best quality (i.e. with the least number of defect structures) were then characterized using a confocal microscope. The average thickness values of the exfoliated layers obtained as a function of shearing frequency were compared to evaluate the effect of shear oscillation on the thickness of the exfoliated graphite sheet. In addition to the thickness measurements, the representative surface morphologies of the exfoliated layers were also characterized optically.

5.3 Results and Discussion

Figure 5.2 shows the effect of shear oscillation frequency on the exfoliated sheet thickness. It can be seen that the average sheet thickness decreases with increase in the frequency. The thickest graphite sheet was obtained at the lowest shearing frequency of 500 Hz and had an average thickness of 25.6 ± 5.4 μm. The thinnest graphite sheet was obtained at the highest applied shearing frequency of 3000 Hz and had an average thickness of 2.8 ±1.6 μm. It is evident that high frequency shear oscillation was more effective in producing thinner layers. On the other hand, increasing the frequency yields sheets with more surface variations as seen in Figure 5.3. Despite the surface variations, the exfoliated layers were of full size (6 x 6 mm^2). Further investigation is required to minimize the surface variations produced at the higher frequency.

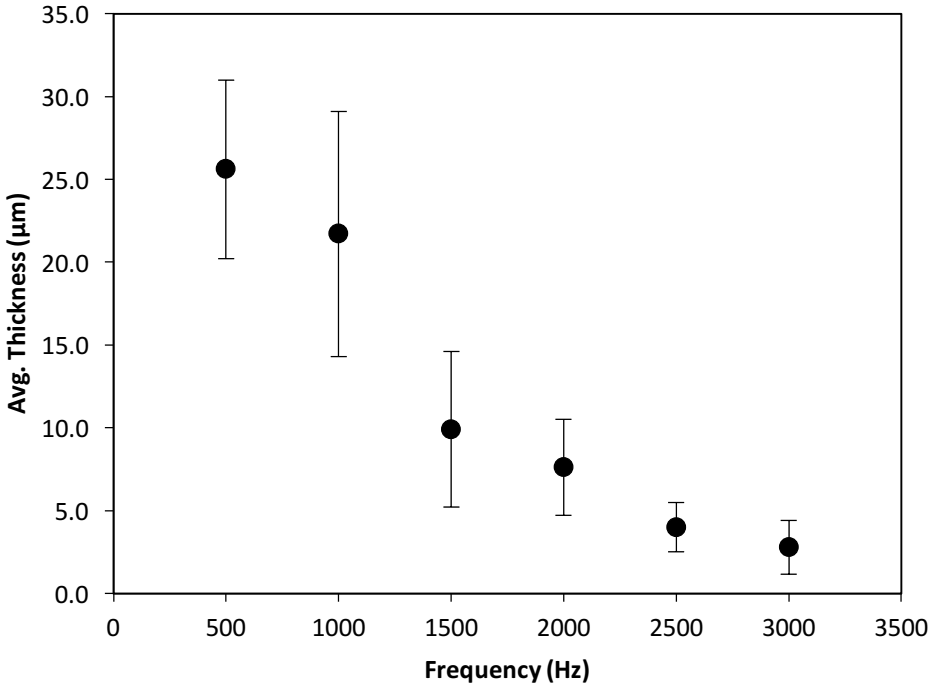

Figure 5.2: Average sheet thickness as a function of shearing frequency

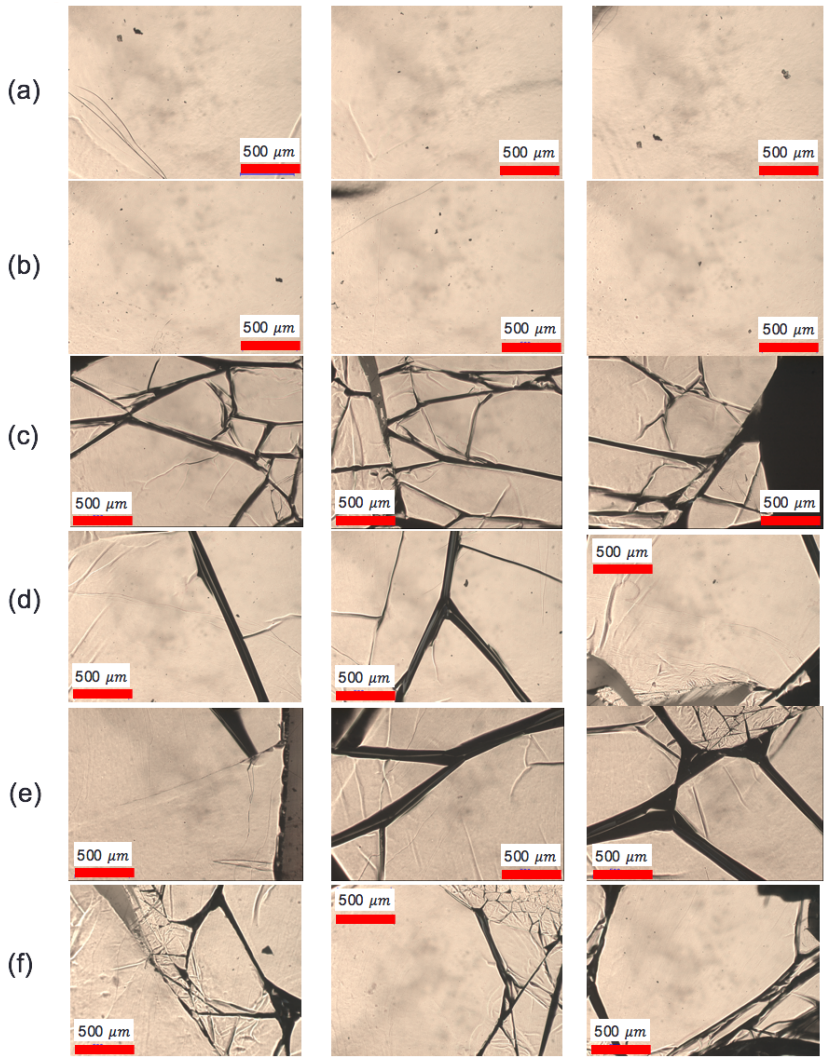

Figure 5.3: Exfoliated layers at different oscillation frequencies: (a) 500 Hz, (b) 1000 Hz, (c) 1500 Hz, (d) 2000 Hz, (e) 2500 Hz, (f) 3000 Hz.

5.4 Summary

This chapter reported a novel experiment designed superpose high frequency shear oscillation into the PDMS-assisted mechanical exfoliation process to exfoliate thinner graphite layers/sheets. The results of the experiment show that high frequency shear oscillation at 3000 Hz, along with a normal contact force of 5N, exfoliation speed of 35 mm/s, and a dwell time of 5 min produced pyrolytic graphite sheets (PGS) that have an average thickness of 2.8 ±1.6 μm and a size of approximately 6 x 6 mm^2. The exfoliated graphite sheets are thinner than the commercially available PGS sheets, which are synthesized by a pyrolysis technique [11]. However, the exfoliated sheets obtained at the higher frequency exhibit greater surface variations. Further work is required to eliminate or minimize these surface variations.

CHAPTER 6. EFFECT OF THICKNESS OF PDMS STAMP ON MECHANICAL EXFOLIATION OF HOPG

6.1 Introduction

As discussed earlier, the lateral elastic deformation of the PDMS stamp was thought to contribute to the formation of surface defects in the exfoliated sheets. To further minimize these defects, the effect of stamp thickness on the exfoliated layers was investigated in this chapter. For this purpose, PDMS was spin coated onto a glass slide to produce thin (< 0.5 mm) uniform PDMS stamp (instead of casting it in the 50 x 50 x 6.25 mm^3 glass container to produce 15 x 15 x 3 mm^3 stamps.) The PDMS-on-glass was then used as a thin stamp to exfoliate sheets from the 12 x 12 mm^2 HOPG sample. The results of this experiment are evaluated to determine the exfoliation process variables that yield layers with the fewest number of surface defects and the highest yield.

6.2 Experimental Procedure

In this experiment, the PDMS stamp was produced using spin coating (SCS G3P8 Spin Coater) to obtain a thin uniform layer of PDMS on a glass substrate. The same procedure described in the previous chapters was followed to mix 10:1 of the PDMS monomer and curing agent, stir the mixture, and then degas it. Once the PDMS mixture was poured into a 50 x 50 x 6.25 mm^3 glass container and quickly transported to the spin coater. A 25 mm x 25 mm x 1 mm glass slide (VWR Microscope Slide) cut with a glass scribe was first placed in the spin coater and then the PDMS mixture was poured onto the glass slide using a pipette. A spin time of 30 s and varying rotational speeds of 2000 rpm, 1500 rpm, 500 rpm, and 300 rpmr were used to prepare different thicknesses of PDMS layers on separate glass slides. After curing in the furnace at 70 °C for 60 min. and post-curing in the freezer, spin-coated PDMS stamps of 38, 111, 236, and 476 μm average

thickness (corresponding to the four spin speeds mentioned above) were obtained. The thickness of each PDMS layer was assessed by sectioning the PDMS-glass assembly into three pieces and then measuring the thickness at three locations along three separate edges of the slide by viewing the section in an optical microscope. Figure 6.1 shows a representative thickness measurement of a sectioned edge of the glass slide. The thickness values obtained using the spin coating process are consistent with prior results obtained using Sylgard-184 PDMS, as shown in Figure 6.2 [50].

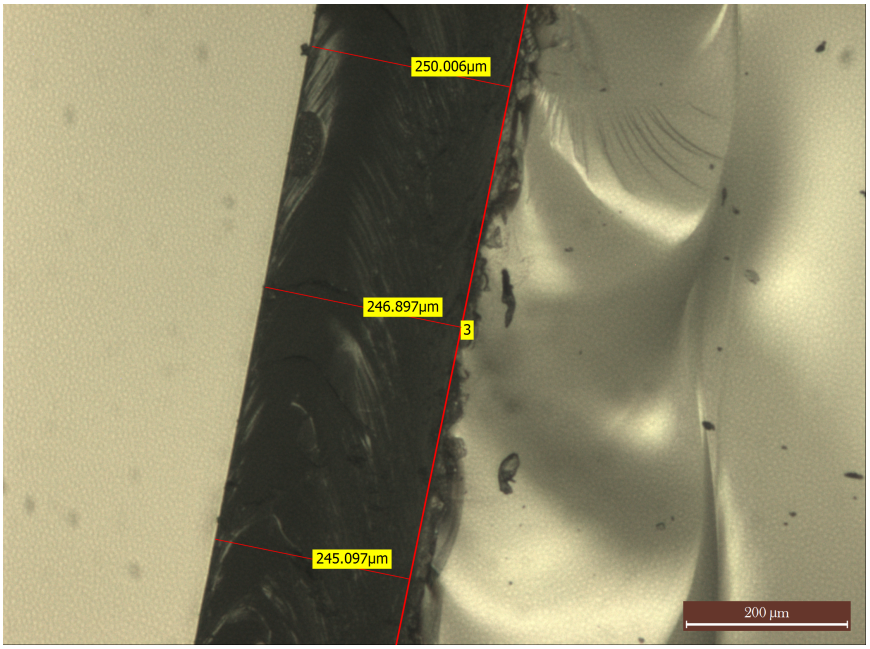

Figure 6.1: Thickness measurement of PDMS spin coated on glass.

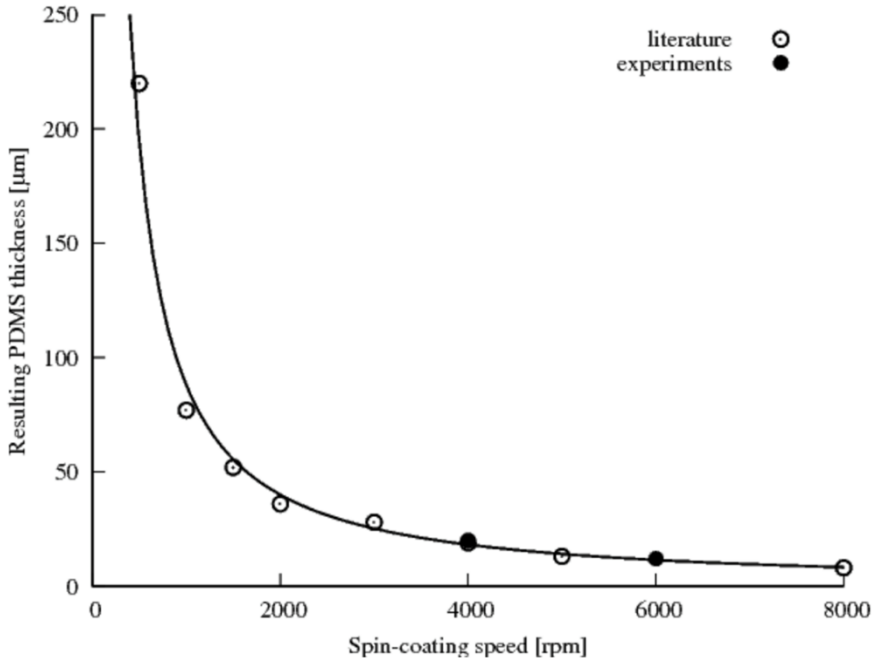

Figure 6.2: Thickness of PDMS as a function of spin coating speed [50].

The spin-coated PDMS stamps were then used to exfoliate the HOPG sample. Exfoliation experiments without shear oscillation were performed by applying a normal contact force of 10 N, a fixed exfoliation speed of 35 mm/s, and a dwell time of 5 min. Two replicates were performed for each run. Once the exfoliation tests were completed, the exfoliated sheets were characterized in terms of their surface area, surface roughness, and surface defects.

6.3 Results and Discussion

Figure 6.3 shows the effect of stamp thickness on the success rate for producing exfoliated sheets with greater than 95% of the intended surface area. Success rate refers to the percentage of experiments that yielded sheets with more than 95% of the nominal HOPG surface area. 100% success rate refers to entire number of repetitions yielding sheets with more than 95 % of intended surface area. It can be seen that a stamp thickness of 236 μm or more is capable of producing exfoliations with surface areas in excess of 95%. For example, the graphite sheet exfoliated using the 236 μm thick PDMS stamp (see Figure 6.4) is equal to the nominal HOPG surface area. Despite some visible surface defect structures and protruding flakes (shown in dark contrast), the exfoliated sheets, including that shown in Figure 6.4, are smoother and have fewer defects than the other layers exfoliated in previous experiments reported in earlier chapters. The experiments performed with PDMS stamps of thickness less than 236 μm yielded incomplete exfoliations of much smaller surface area.

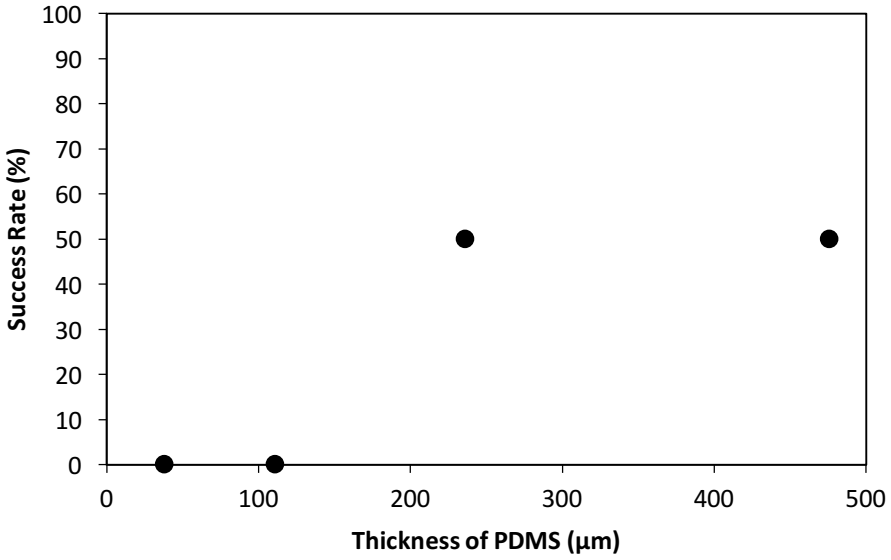

Figure 6.3: Effect of stamp thickness on successfully exfoliating sheets with greater than 95% of the intended surface area.

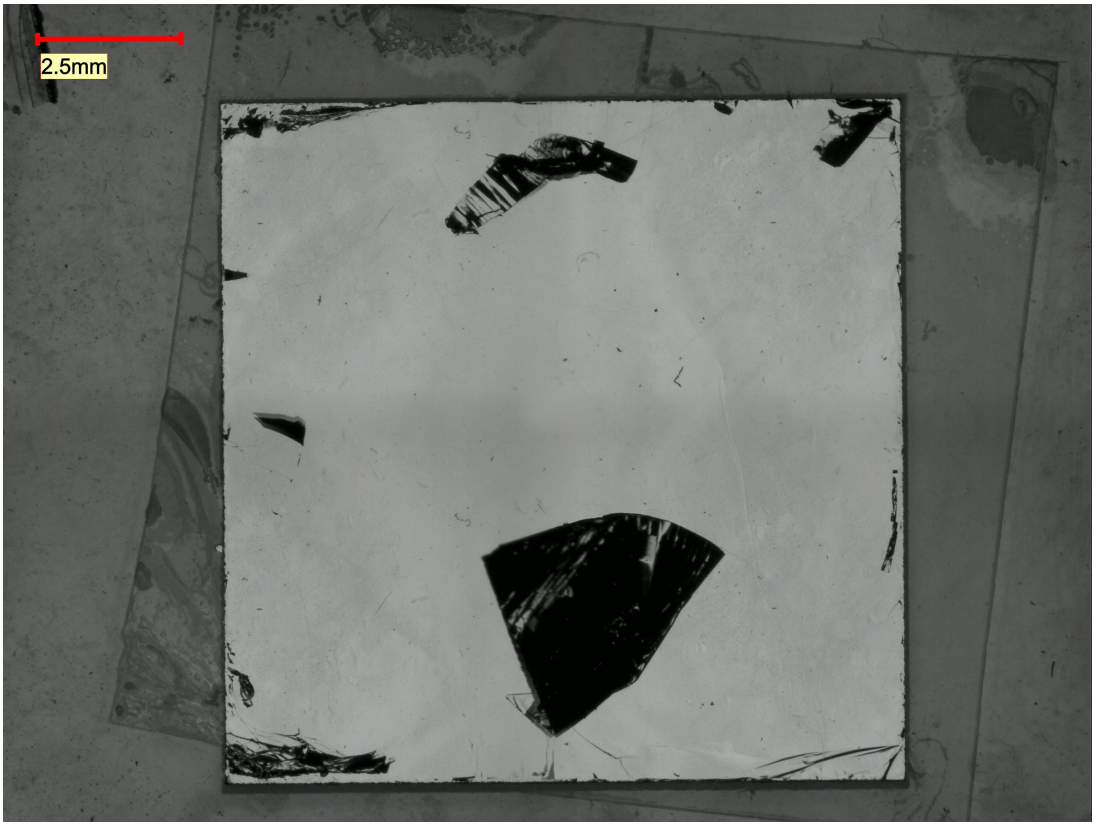

Figure 6.4: Exfoliated pyrolytic graphite sheet produced by the 236 µm thick PDMS stamp.

Figure 6.5 compares the characteristic surface morphologies of the sheets exfoliated using the 236 µm thick and 476 µm thick PDMS stamps. The exfoliated layers obtained with the 236 µm PDMS stamp have an average arithmetic surface roughness of 0.17 ± 0.11 µm. The exfoliated layers obtained by the 476 µm thick PDMS stamp have a larger average arithmetic surface roughness of 0.25 ± 0.25 µm. As shown in Figure 6.5, the exfoliated layers obtained with the 476 µm thick PDMS stamp displays more and larger defect structures. In addition, the graphite sheet obtained with the 476 µm thick PDMS stamp had a large portion of its surface protruding from the PDMS stamp at an incline (not shown here,) whereas the other sheets lie flat on the PDMS (Figure 6.4). Therefore, the 236 µm thick stamp was found to yield the best results measured in terms of success rate and sheet quality.

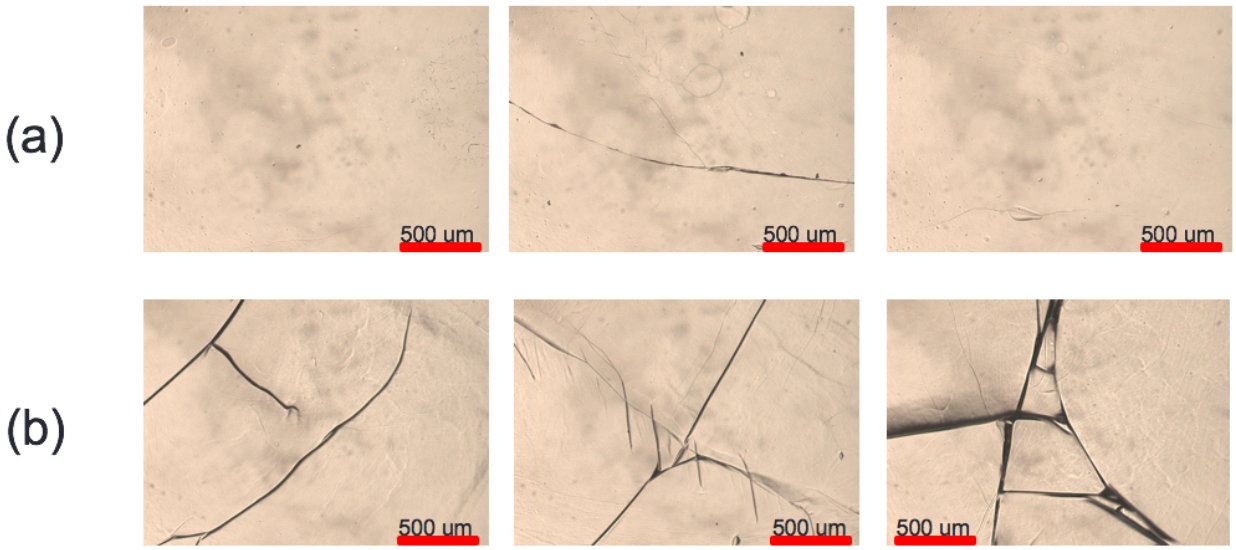

Figure 6.5: Exfoliated sheet morphologies for PDMS stamp thicknesses of (a) 236 µm, and (b) 476 µm.

6.4 Summary

In this chapter, PDMS was spin-coated onto a glass slide to produce PDMS stamps with different thicknesses of 38, 111, 236, and 476 µm. These stamps were used in the mechanical exfoliation of HOPG to show that a certain range of PDMS thickness allows higher yield and fewer defects. Specifically, the exfoliated pyrolytic graphite sheet obtained with the 236 µm thick PDMS stamp had smoothest surface and the smallest number of defects than any other layers obtained by far. These observations indicate that optimization of PDMS stamp thickness is crucial for obtaining high quality graphite sheets. In the following chapter, this type of PDMS stamp is combined with high frequency shear oscillation (discussed in Chapter 5) to assess the feasibility of exfoliating large area, thin graphite sheets with minimal surface defects.

CHAPTER 7. EFFECT OF BEST CONDITIONS ON MECHANICAL EXFOLIATION OF HOPG

7.1 Introduction

The two experiments discussed in Chapter 5 and Chapter 6 showed that high frequency shear oscillation produced thinner HOPG layers and that an optimum thickness of PDMS yielded higher layer quality, respectively. Consequently, an experiment was then designed to evaluate the combined effect of shear oscillation and the use of a thin PDMS stamp. This experiment, which is discussed in detail in the following sections, produced by far the thinnest HOPG sheets with fewer defects and larger size (surface area). The quality and properties (electrical and thermal) of these layers were characterized using the following methods: (1) micro-Raman spectroscopy was used to analyze the Raman spectra of the exfoliated layers [28, 48, 51], (2) the four-point probe method was used to determine the sheet resistivity of the exfoliated layers [52-54], and (3) the time domain thermoreflectance (TDTR) technique [55-57] was used to measure the in-plane thermal conductivity of the exfoliated layers.

7.2 Experimental Procedure

PDMS stamps were prepared in the same way they were prepared in Chapter 6. The thickness of the PDMS layer spin-coated on glass was 236 μm because, in prior experiments, it yielded exfoliated layers with fewer defects and full areal coverage. This stamp was used in the mechanical exfoliation of HOPG performed on the experimental setup discussed in Chapter 5 (see Figure 5.1). To accommodate shear-based oscillation, the HOPG was again cleaved into 6 x 6 mm^2 squares. A shear oscillation frequency of 3000 Hz was used to exfoliate the HOPG because it produced the thinnest sheet in prior experiments reported in Chapter 5. Because the size of the

HOPG was reduced, two different normal contact forces were initially used to find process parameters that produce thinner HOPG layers with fewer defects and complete surface area (equal to the size of the starting HOPG sample).

Two different normal contact forces of 5 N and 7.5 N were used in this experiment. The 5 N force was chosen because previous shearing experiments showed that this normal contact force repeatedly exfoliated complete and thin layers from the HOPG. The 7.5 N force was chosen because it represents the average of the force applied in the thin PDMS experiment (10 N) and the force applied in the shear oscillation experiment (5 N). The other exfoliation parameters, including the shear oscillation frequency, exfoliation speed, and dwell time were 3000 Hz, 35 mm/s, and 5 min., respectively.

The thinnest HOPG layers obtained in this experiment were characterized using micro-Raman spectroscopy, the four-point probe method, and the TDTR. Micro-Raman spectroscopy is widely used to characterize single-layer or few-layer graphene [48, 51]. Although the exfoliated layers obtained in the current experiment were thicker, it is still possible to check for existence of intrinsic defects in the exfoliated layers using the Raman spectra. Raman scattering from the micro-Raman spectroscopy (HORIBA Jobin-Yvon LabRAM HR800) was excited by $\lambda = 532$ nm with the laser beam size of ~1 μm^2. The four-point probe method was used to measure the electrical sheet resistance of the exfoliated layers. The 7 method was used to measure thermal conductivity of the exfoliated layers by heating the thin graphite layer with a laser pulse and measuring its temperature decay through changes in reflectivity. The TDTR technique is more thoroughly described in the following paragraph.

TDTR is an optical pump-probe technique that heats the surface of a sample using an ultrafast laser and then monitors the change in reflectivity of a thin metal layer on 10the sample to

measure temperature. The combination of a sub-picosecond pulse-width and a precision mechanical delay stage allows the system to characterize the temperature response over short timescales, 0.1 to 7 ns. The temperature response of the surface is fitted to a radial 2D diffusive heat transfer model to determine the thermal conductivity and the thermal boundary conductance values [55]. The pump (heating) laser is modulated to alter the penetration depth into the sample and change the sensitivity of the heat transfer model to different parameters. In this work modulation frequencies of 2.2 and 3.6 MHz were used. By changing the heating frequency, the sensitivity to the in-plane and through-thickness thermal conductivities of the graphite sheet was altered. The sensitivity (described in more detail in the literature [55]) is shown in Figure 7.1.

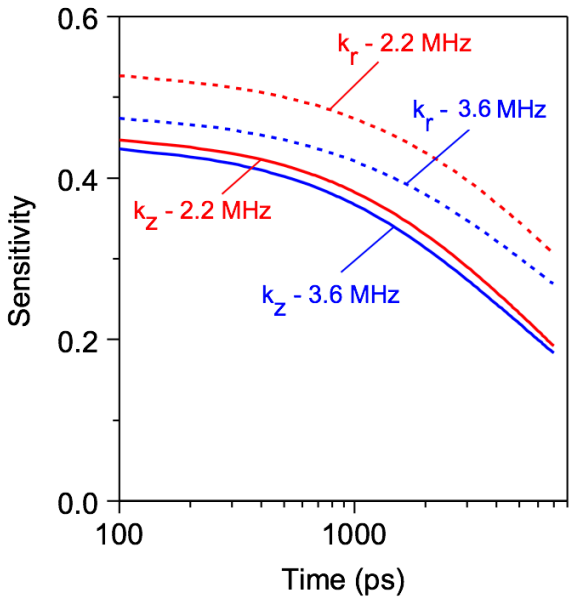

Figure 7.1: Sensitivity to in-plane (k_r) and through-plane (k_z) thermal conductivity at different modulation frequencies.

Prior to measurement, a thin (~100 nm) Al film was deposited on the surface of the exfoliated graphite sheet to act as a temperature transducer; Al has a relatively high coefficient of

thermoreflectance at the probe wavelength of 800 nm, enabling a good signal-to-noise ratio. By simultaneously fitting the data at two different heating frequencies, both the in-plane and through-thickness thermal conductivities of the graphite sheet were determined. An example of the data fit is shown in Figure 7.2. In this plot the y-axis label (V_{in}/V_{out}) is simply the ratio of the real and imaginary temperature signals from the lock-in amplifier and is the preferred method of showing the temperature response for TDTR since it contains more information that the amplitude [56].

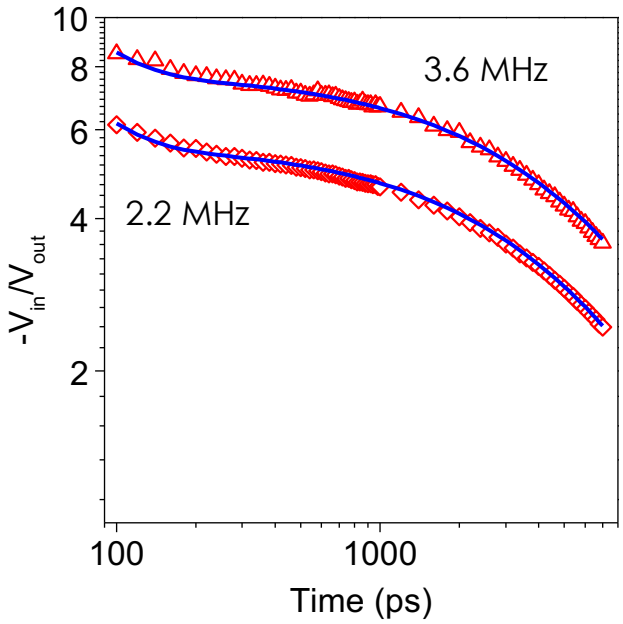

Figure 7.2: TDTR data fit for graphite sheet at two frequencies.

The uncertainty in the TDTR measurements was determined using a Monte Carlo technique described elsewhere [57]. The simulation was run for 1,000 iterations with the main sources of error coming from uncertainty in the Al layer thickness (5%) and the laser spot size (10%). The exfoliation and characterization results of this experiment are reported and discussed in the next section.

7.3 Results and Discussion

The two normal contact forces produced different exfoliation results. Only 1 in 8 trials with the 5N contact force yielded sheets with more than 80% surface area. On the other hand, 100% of the trials performed at 7.5 N contact force yielded sheets with almost full surface areas. Figure 7.3 shows images of the two thinnest layers obtained with the 236 µm thick PDMS stamp at 7.5 N contact force and 3000 Hz shear oscillation frequency. Figure 7.4 shows the representative surface morphologies of the two exfoliated sheets. Three images were taken at three different locations on each surface. The average thicknesses of the two exfoliated layers were 0.88± 0.74 µm (Figure 7.3a) and 0.83 ± 0.42 µm (Figure 7.3b), respectively. As shown in Figure 7.5, these layers are the thinnest and of almost full areal coverage among all the exfoliation experiments discussed in the thesis thus far. Some regions of the exfoliated sheets had a thickness less than 0.4 µm. This clearly shows that the combined use of shear oscillation at high frequency and the use of a thin PDMS stamp yields the best exfoliation results.

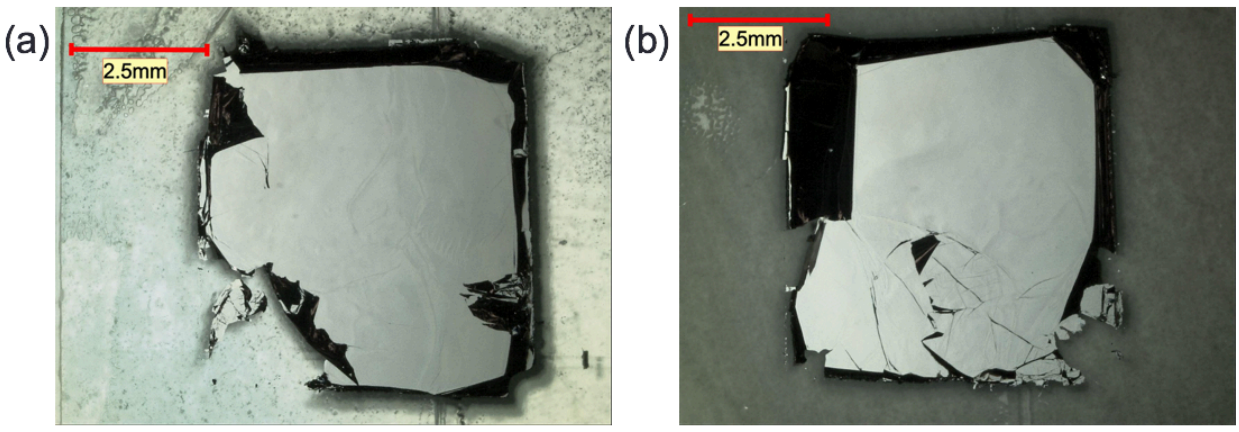

Figure 7.3: (a) Exfoliated sheet number 1, and (b) exfoliated sheet number 2 via thin PDMS stamp (236 µm) and shear oscillation (3000 Hz, ±1 µm amplitude).

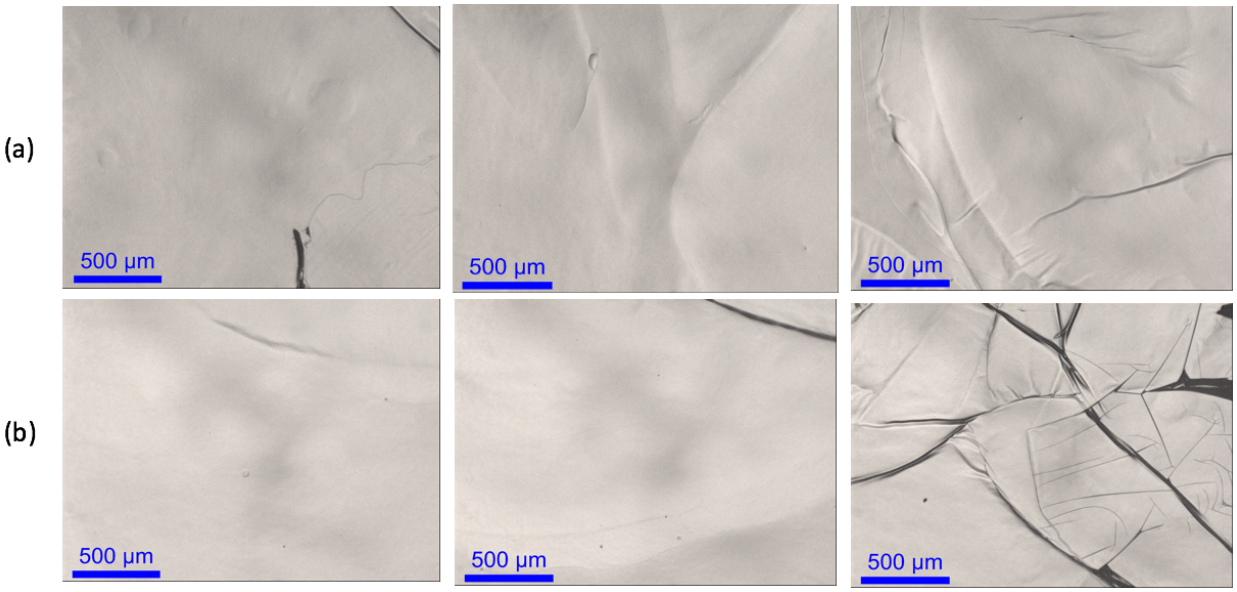

Figure 7.4: Surface morphologies of exfoliated sheets obtained using the thin PDMS stamp (236 µm) and shear oscillation (3000 Hz, ±1 µm amplitude); (a) exfoliated sample 1 and (b) exfoliated sample 2.

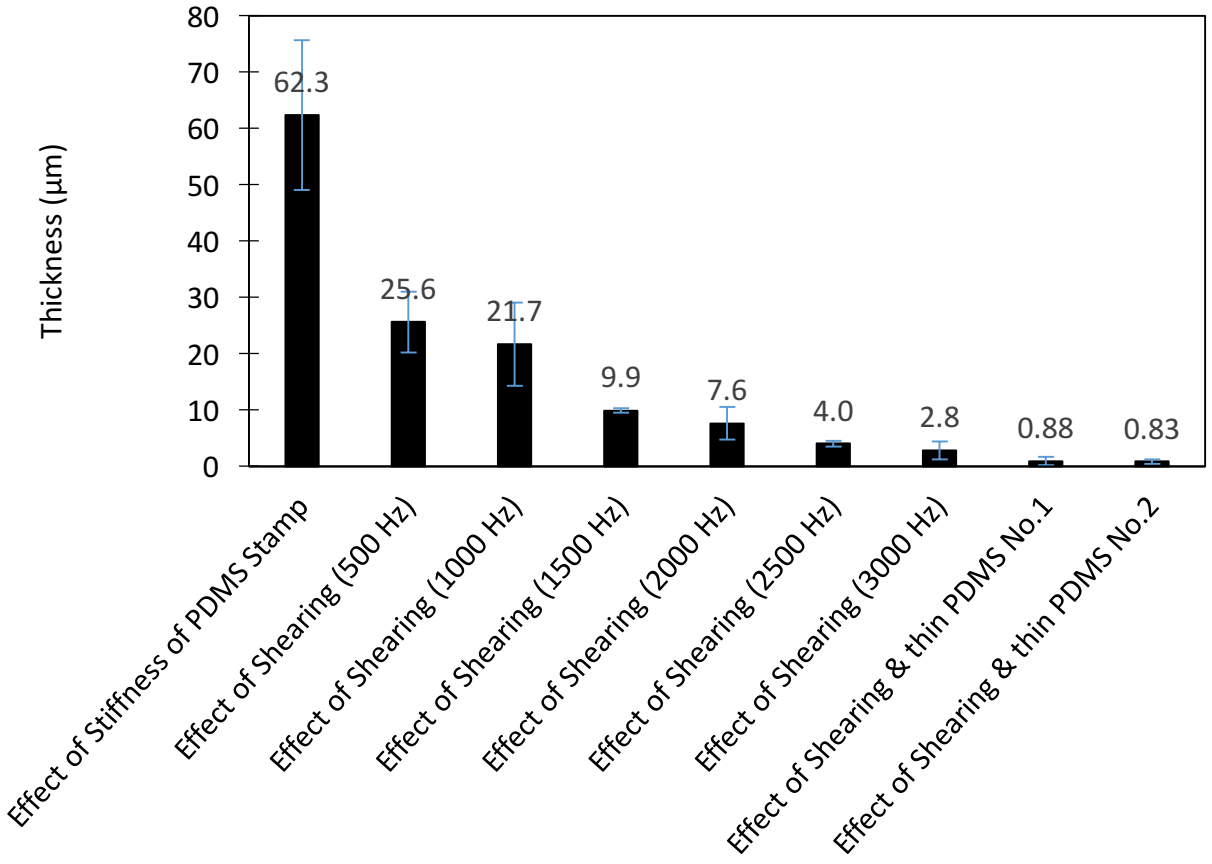

Figure 7.5: Comparison of sheet thicknesses obtained under different conditions.

The four-point probe electrical sheet resistivity characterization of the 0.88 ± 0.74 µm thick graphite sheet yielded a sheet resistance of 0.22 ohm per square for the entire exfoliated layer (including the ridges at the corners) and a sheet resistance of 0.12 ohm per square for the flat region only (i.e. excluding the ridges near the corners). These sheet resistance values were then converted to the electrical conductance of the exfoliated sheet, using Pouillet's law (see Equation (4)) and the equations for sheet resistance [54]:

$$R = \frac{\rho L}{A} \tag{1}$$

$$R_{sh} = \frac{\rho}{t} \tag{2}$$

$$R = R_{sh} * \frac{L}{W} \tag{3}$$

$$\sigma = \frac{1}{\rho} \tag{4}$$

where:

R - electrical resistance

ρ - resistivity

L – sheet length

A - cross-sectional area

R_{sh} - sheet resistance (ohm per square)

t – sheet thickness

W- sheet width

σ – conductivity (S/cm)

The electrical conductivity values thus obtained are listed in Table 7.1 and compared with the electrical conductivities of three commercially available PGS sheets and the original HOPG [11, 58]. The electrical conductivities, regardless of where the sheet resistance was measured (i.e. in the flat region or in the entire sheet), are substantially higher than the values reported for commercially available PGS sheets of different thicknesses, as shown in Figure 7.6. This result

suggests that the mechanical exfoliation process developed in this thesis is capable of producing thinner graphite sheets that exhibit much higher electrical conductivities.

Table 7.1: Electrical conductivities of HOPG, exfoliated sheet, and various PGS sheets.

	Approximate Size (mm x mm)	Thickness (μm)	Electrical Conductivity (S/cm)
Original HOPG (Grade ZYA, SPI Supplies)	12 x 12	2000	25000
Entire film of exfoliated sheet number 1 (with a ridge in one corner)	6 x 6	0.88	52000
Flat region of exfoliated sheet number 1	6 x 6	0.88	95000
PGS (Panasonic PGS)	90 x 90	25	20000
PGS (Panasonic PGS)	90 x 90	70	10000
PGS (Panasonic PGS)	90 x 90	100	10000

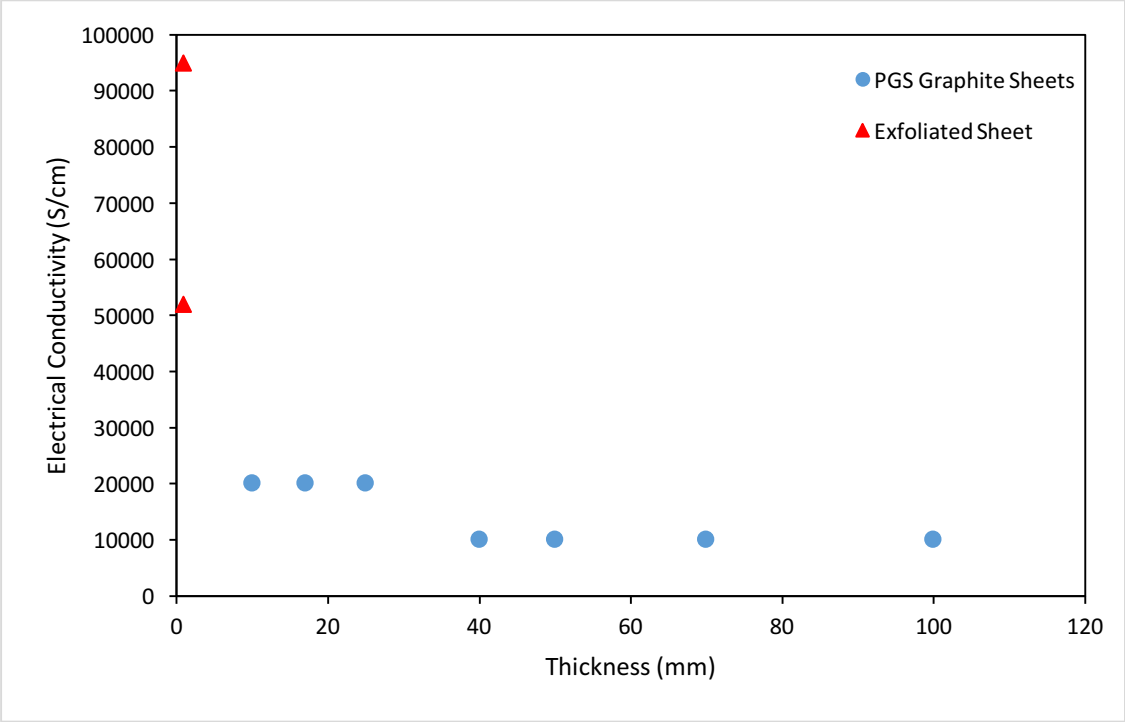

Figure 7.6: Electrical conductivities of the exfoliated HOPG sheet and commercially available PGS sheets of varying thickness.

The thermal conductivities of the thin exfoliated graphite samples (Sample 1 & Sample 2 in Figure 7.3 were measured using the TDTR method. Each exfoliated graphite sheet sample was measured at three separate spots and the results are shown in Table 7.2.

Table 7.2: Thermal conductivity measurement summary.

	Thermal Conductivity, W/m-K					
	Through-plane			**In-plane**		
Sample 1, Spot 1	6.80	±	0.82	1978	±	237
Sample 1, Spot 2	5.26	±	0.53	1979	±	317
Sample 2, Spot 1	6.25	±	0.63	2267	±	204
Sample 2, Spot 2	4.16	±	1.04	2312	±	439

Thermal conductivity data for commercially available PGS sheets of thicknesses ranging from 10 µm to 100 µm are given in Table 7.3. It can be seen that the in-plane thermal conductivities of the thinner and smaller surface area mechanically exfoliated graphite sheets are higher than the X-Y direction (in-plane) thermal conductivities of the commercially available PGS sheets of varying thickness, as shown in Figure 7.7. The extrapolation of the fitted curve for PGS at the same thickness (.83 µm) lies below the thermal conductivity of the exfoliated sheet. These results suggest that the mechanically exfoliated thin graphite sheets can be useful for high efficiency heat sink applications.

Table 7.3 Properties of commercially available PGS [11].

MATERIAL CHARACTERISTICS OF PGS GRAPHITE SHEETS								
		10 µm	17 µm	25 µm	40 µm	50 µm	70 µm	100 µm
Thickness (mm)		0.010 ± 0.002	0.017 ± 0.005	0.025 ± 0.010	0.040 ± 0.012	0.050 ± 0.015	0.070 ± 0.015	0.100 ± 0.030
Thermal conductivity (W/mK)	X-Y direction	1900	1750	1600	1350	1300	1000	700
	Z direction	(10)	(11)	(18)	(20)	(20)	(20)	(26)
Thermal diffusivity, cm^2/s (m^2/s)		10 to 12 (0.001 to 0.0012)	10 to 11 (0.001 to 0.0011)	9 to 10 (0.009 to 0.001)	9 to 10 (0.009 to 0.001)	8 to 10 (0.008 to 0.001)	8 to 10 (0.008 to 0.001)	8 to 10 (0.008 to 0.001)
Density, g/cm^3 (kg/m^3)		2.13 (2130)	2.10 (2100)	1.95 (1950)	1.80 (1800)	1.70 (1700)	1.21 (1210)	0.85 (850)
Specific heat at 50°C (J/kgK)		0.85 (850)	0.85 (850)	0.85 (850)	0.85 (850)	0.85 (850)	0.85 (850)	0.85 (850)
Heat resistance, °C		400	400	400	400	400	400	400
Extensional strength (MPa)	X-Y direction	40	40	30	25	20	20	20
	Z direction	0.1	0.1	0.1	0.4	0.4	0.4	0.4
Bending test, R5/180° (times)		30,000 or more	30,000 or more	30,000 or more	30,000 or more	30,000 or more	30,000 or more	30,000 or more
Electric conductivity, S/cm (S/m)		20,000 (2.0×10^6)	20,000 (2.0×10^6)	20,000 (2.0×10^6)	10,000 (1.0×10^6)	10,000 (1.0×10^6)	10,000 (1.0×10^6)	10,000 (1.0×10^6)

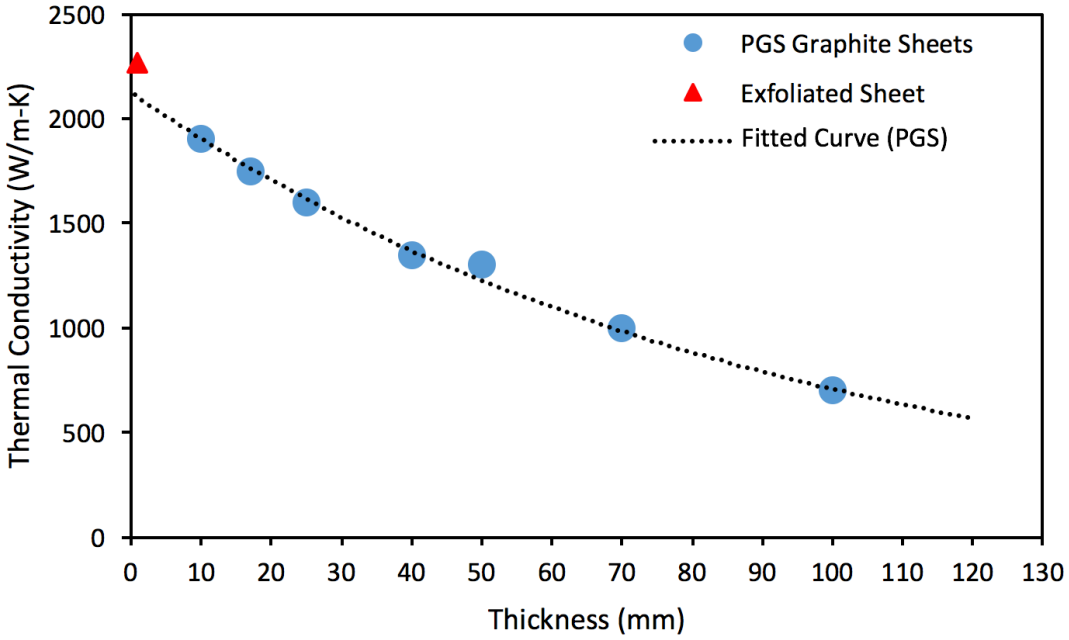

Figure 7.7: Thermal conductivities of the exfoliated HOPG sheet and commercially available PGS sheets of varying thickness.

Micro-Raman spectroscopy was performed on another exfoliated sheet of similar thickness (1.25 ± 0.42 μm) obtained from the same experiment. The Raman spectra was obtained at six different locations of the sample which comprised of three flat regions and three ridges. The Raman spectra shown in Figure 7.8 exhibits the typical spectra of HOPG/graphene (regardless of the different regions). The presence of the G peak (1580 cm^{-1}) and 2D peak (2670 cm^{-1}), typical of HOPG/graphene, can be seen in the spectra [28, 59]. In addition, there is no D peak at ~1350 cm^{-1}, suggesting that the mechanically exfoliated graphite layers do not have any intrinsic defects caused by discontinuity in the carbon network, which are often present in CVD grown graphene [28]. Thus, these spectra show that mechanical exfoliation using a thin PDMS stamp combined with high frequency shear oscillation produces relatively defect-free layers.

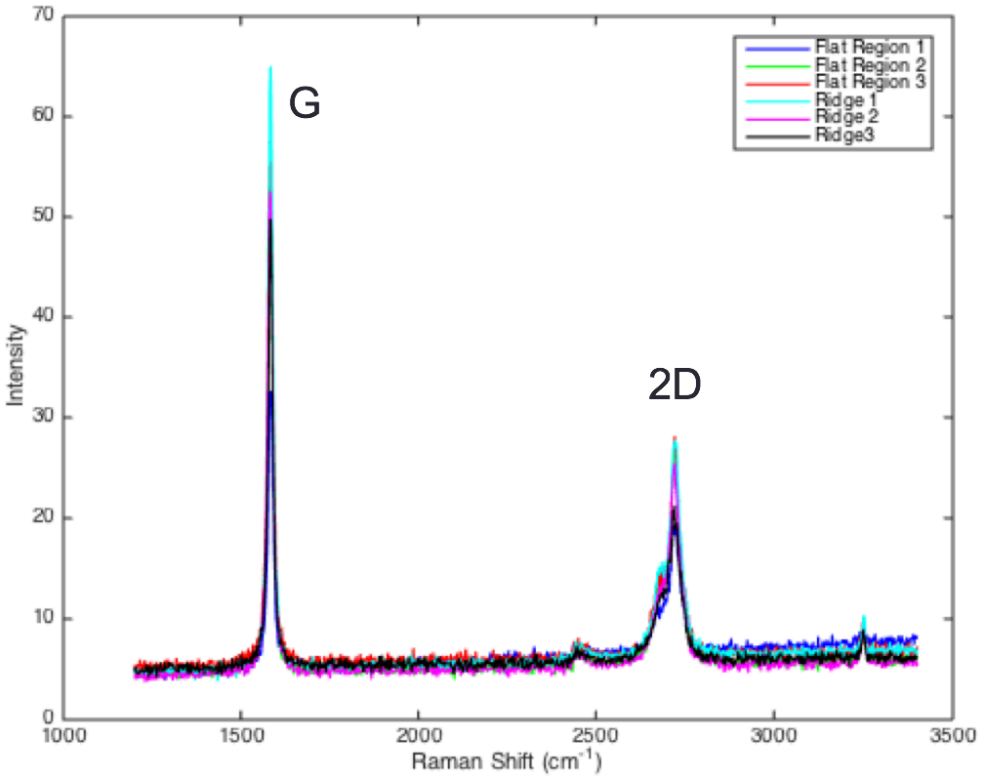

Figure 7.8: Raman spectra of the 1.25 ± 0.42 µm thick exfoliated layer.

7.4 Summary

This chapter showed that the use of the "best" mechanical exfoliation conditions consisting of a thin uniform PDMS stamp and high frequency shear oscillation produced the thinnest graphite layers with the largest surface areas. The average thicknesses of the two thinnest sheets obtained were 0.88± 0.74 µm and 0.83 ± 0.42 µm. Characterization of the exfoliated layers using Raman spectroscopy showed that the layers were of high quality with no intrinsic defects in them. Electrical conductivity and thermal conductivity measurements of the exfoliated sheets yielded higher electrical and thermal conductivity values than those reported for commercially available pyrolytic graphite sheets. These superior properties of the exfoliated sheets, along with their greater flexibility, suggest that these sheets can serve as a more efficient electrical conductor and/or heat sink material for various applications discussed in the literature review, e.g. PEMFC [10].

CHAPTER 8. EFFECT OF HOPG SURFACE AREA ON MECHANICAL EXFOLIATION

8.1 Introduction

Prior research on mechanical exfoliation of graphene involved fabricating small patterned mesas or micro-pillars on top of the HOPG and exfoliating the exposed surface of mesas ranging in size from approximately 6 x 6 μm^2 to 40 x 40 μm^2 by directly transferring them to a SiO_2 surface [40, 42-44]. This procedure was shown to produce mono- or few-layer graphene, albeit it was characterized by inconsistencies in yield and size of the exfoliated layers. As noted earlier, prior work acknowledges that producing uniformly large area mono- or few-layer graphene will require better stamp engineering and stamping methods [42]. Hence, this chapter seeks to evaluate the scalability of the HOPG mesa-based exfoliation approach. Note that the experiments reported in this chapter do not involve shear oscillation.

8.2 Experimental Procedure

A regular pattern of mesas or micro-pillars of 500 x 500 μm^2 size were created via a photolithography process. Figure 8.1 illustrates the general steps used to etch the HOPG and to make the patterned mesas.

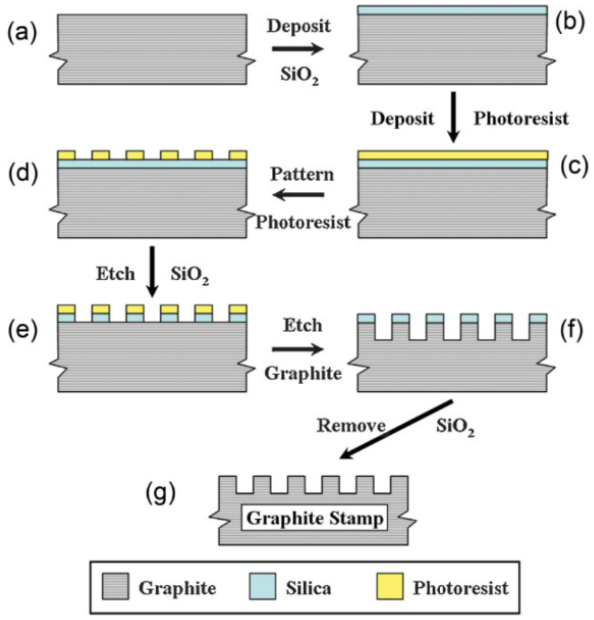

Figure 8.1: Process of preparing mesas on HOPG [42].

A mask containing a regular pattern of 500 x 500 μm^2 squares equally spaced over a 15 x 15 mm^2 area was prepared using photolithography. The first step of this process involved depositing SiO_2 on the HOPG block. Deposition of 300 nm of SiO_2 on the graphite sample was accomplished by plasma-enhanced chemical vapor deposition (PECVD) (Oxford Plasmalab 80 Plus). The SiO_2 layer served as a sacrificial layer during subsequent etching of the HOPG. A negative photoresist (Futurrex NR9-1500PY) was spin-coated at 1500 rpm for 40 seconds. The negative photoresist was then baked at 150 °C for 100 seconds to ensure the photoresist was rigidly attached to the HOPG. After baking, the HOPG sample was attached to a 100 mm diameter silicon wafer via Kapton tape to ensure the wafer fit flush into the subsequent photolithography tools. The next step involved a mask aligner (Karl Suss MA-6). Prior to placing the sample into the mask aligner, an ultraviolet (UV) intensity of 350W was generated in the mask aligner via a 365nm wavelength mercury lamp to calculate the exposure time needed. The exposure time was calculated by dividing the required energy dose (about 335 mJ/cm^2-s) by the intensity. Once the exposure

time was set, the mask and the wafer containing the sample were placed in the mask aligner to align the mesa pattern onto the sample. The alignment did not have to be perfectly parallel to the original HOPG surface because the exact location of the 500 x 500 μm^2 mesa pattern on the HOPG was not critical for the purposes of this study. After aligning the mask, the photoresist was exposed to UV light through the mask. The exposed photoresist then underwent another baking process (post-exposure baking) at 100 °C for 100 seconds. Since this is a negative photoresist, UV exposure polymerizes the exposed resist surrounding the mesas thereby making its dissolution difficult. After the post-baking step, a lift-off process was performed by dipping the sample into the resist developer (Futurrex RD6), which lifted-off only the unexposed region. This step created square mesas of photoresist on the SiO_2-deposited HOPG, as shown in Figure 8.2.

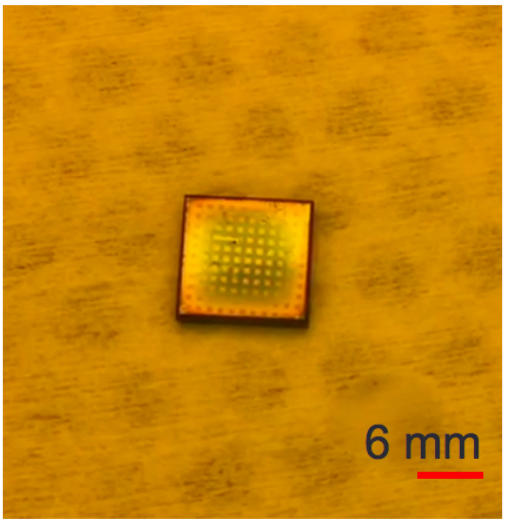

Figure 8.2: A regular pattern of photoresist on HOPG.

The next step involved etching of SiO_2 and the HOPG. After development of the resist, the remaining resist pattern was used as a sacrificial layer for etching the SiO_2. A reactive ion etching (RIE) plasma system (Vision 320 RIE) was used to etch away the 300 nm of SiO_2 that was not covered by the developed photoresist pattern. After etching SiO_2, the sample was soaked in acetone

to remove the square pattern of negative photoresist. The structure left in the HOPG sample was a square mesa pattern with SiO_2 deposited on top of the mesas. The SiO_2 protected the HOPG from etching the complete surface away. In the last step, the sample was placed in a inductively coupled plasma (ICP) system (STS AOE ICP) with an advanced oxide etch (AOE) source to etch the HOPG that was not covered by the patterned sacrificial layer of SiO_2. To accomplish this etching step, 40 standard cubic centimeter per minute (sccm) of O_2, 20 sccm of CO_2, 1500 W of coil power, and 200 W of platen power were applied. After etching the HOPG, the standard oxide etching process was again used to etch away the remaining patterned SiO_2. This final step of the photolithography process flow resulted in square mesas on the HOPG sample. The mesas were then characterized using an optical profilometer (Zygo ZeGage) and a contact stylus profilometer (Tencor P15). The average height of the mesas was determined to be 6.30 ± 0.25 μm. Figure 8.3 shows an optical microscope image of the HOPG mesas. This sample was then used as the HOPG source for PDMS-based mechanical exfoliation.

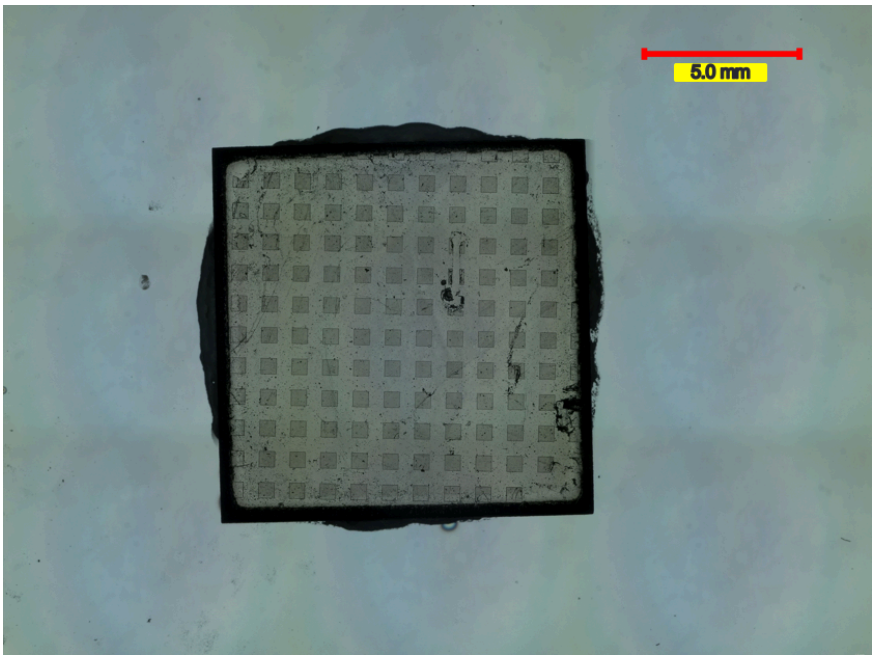

Figure 8.3: A regular pattern of square graphite mesas on HOPG.

Initially, systematic mechanical exfoliation of the mesas using the PDMS stamp based process discussed earlier in the thesis was attempted. The exfoliation process conditions consisted of a very low contact force of 0.2 N, 35 mm/s exfoliation speed, and a 5 min. dwell time. An extremely low contact force was used to minimize the penetration of the compliant PDMS into the gaps between the mesas. However, these conditions did not result in successful exfoliation of 2D layers from the mesas. Therefore, manual exfoliation of the mesas was attempted to determine if mono- or few-layer graphene could be obtained. In the manual exfoliation attempt, a thin PDMS stamp of 236 μm average thickness was pressed against the mesas and subsequently lifted using a peeling action. Albeit less controlled than the prior exfoliation experiments performed using the apparatus shown in Figure 3.1a, the manual process nevertheless yielded successful exfoliation of a few mesas. Consecutive manual press-and-peel trials were performed on the few mesas exfoliated by the first stamping operation. This trial and error process resulted in two very thin layers shown in Figure 8.4. These layers were thinner than any 2D graphite layer obtained in the prior experiments discussed in this thesis. These thin layers were selected for further characterization.

8.3 Results and Discussions

As discussed above, the manual exfoliation process using the HOPG mesas produced two layers that were thinner than the thinnest 2D layer exfoliated in prior experiments presented in this thesis. The first sample (Figure 8.4a) had an average thickness of 0.462 ± 0.180 μm while the second sample (Figure 8.4b) had an average thickness 0.515 ± 0.163 μm. Due to the repeated peeling process used, the areal sizes of these layers were smaller than the original 500 x 500 μm^2 areas of the individual mesas in the pattern. Raman spectra of the layers (also shown in Figure 8.4) are consistent with the Raman spectrum of HOPG reported earlier in Figure 7.8. As discussed earlier, the absence of the D peak (1360 cm^{-1}) suggests that these layers do not have significant intrinsic defects or discontinuity in the carbon network.

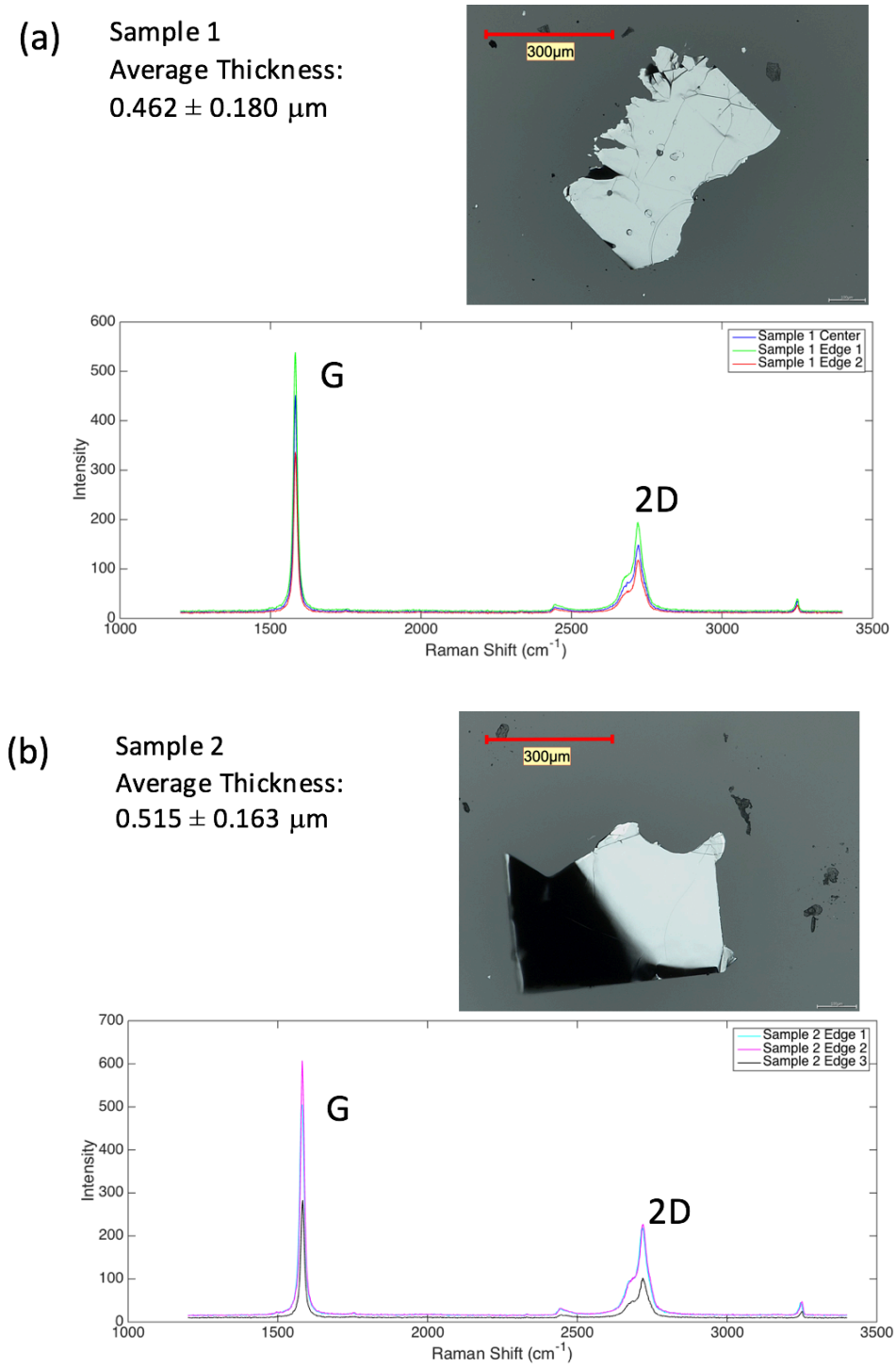

Figure 8.4: (a) Sample 1 and (b) Sample 2 exfoliated layers from mesas and their characterization results.

8.4 Summary

This chapter presented results of a preliminary investigation of the scalability of a HOPG mesa based mechanical exfoliation approach. Despite the limitations of the eventual manual exfoliation process used to partially exfoliate thin graphite layers from the HOPG mesas, the results showed that PDMS-assisted mechanical exfoliation is capable of further reducing the thickness of the exfoliated layers. While only partial exfoliation of the mesas was realized using the manual exfoliation process, the exfoliated layers obtained were still larger than those reported in the literature for this process [42, 43]. These results suggest that the use of the PDMS stamp based mechanical exfoliation process on HOPG mesas may be scalable but that further work is needed to realize a well-controlled and repeatable process.

CHAPTER 9. CONCLUSIONS AND RECOMMENDATIONS

9.1 Conclusions

The main conclusions of this thesis are as follows:

Effect of the PDMS stamp curing time on the exfoliation process and on the layers exfoliated from the HOPG:

1. An optimum PDMS stamp curing time of 60 min. held at 70^0C curing temperature yielded the best results for mechanical exfoliation of HOPG. Using these curing conditions along with a normal contact force of 10 N, a dwell time of 5 min., and an exfoliation speed of 30 mm/s, produced 62.3 ± 13.3 μm thick sheet with relatively less number of defects while possessing full areal coverage (12 x 12 mm^2). Determination of the optimum PDMS stamp curing time is important in mechanically exfoliating high quality HOPG layers/sheets

Effect of surface roughness of the initial HOPG source on the exfoliation process:

2. The initial HOPG surface condition/roughness has significant impact on the mechanical exfoliation process using the PDMS stamp. In general, a smoother HOPG surface produced higher yield during the process. An initial HOPG average arithmetic surface roughness less than 0.24 μm yielded full-area exfoliated graphite sheets with relatively low surface roughness, which can also be manually transferred onto a Si/SiO_2 wafer.

Effect of high frequency in-plane (shear) oscillation on the exfoliation process and on the resulting 2D graphite layers:

3. Superposition of a high frequency shearing oscillation onto the normal mechanical exfoliation process yielded thinner exfoliated sheets. Specifically, high frequency shear oscillation at 3000 Hz, along with a normal contact force of 5 N, a dwell time of 5 min., and an exfoliation speed of 35 mm/s, produced the thinnest (2.8 ±1.6 μm) full-area (6 x 6 mm^2) HOPG layers.

Effect of PDMS stamp thickness on the exfoliation process and on the resulting 2D graphite layers:

4. Use of the optimum PDMS stamp thickness produced large area (12 x 12 mm^2) exfoliated layers with fewer defects and with greater repeatability. The exfoliated pyrolytic graphite sheet obtained with the 236 μm thick PDMS stamp had the lowest surface roughness and had the least number of defects. Determination of the optimum PDMS stamp thickness is important in mechanically exfoliating high quality HOPG layers/sheets.

Combination of exfoliation process parameters that yield the thinnest 2D graphite layers:

5. The combination of high frequency shear oscillation (at 3000 Hz) and a thin (236 μm) uniform PDMS stamp produced the thinnest sheets (0.83 ± 0.42 μm) with full areal coverage at a normal contact force of 7.5 N, dwell time of 5 min., and an exfoliation speed of 35 mm/s. Electrical and thermal characterization of the thin sheets showed that they are thinner, of high quality (no D-peak in the Raman spectra), and electrically and thermally more conductive than commercially available PGS sheets. Specifically, the exfoliated sheets were found to have a sheet resistance of 0.12 ohm per square and a maximum in-plane thermal conductivity of 2312 ± 439 W/m-K.

9.2 Recommendations for Future Work

Future work should be performed to determine the process conditions required to produce graphite layers thinner than the minimum (0.83 ± 0.42 μm) found in the current work. Specifically, advanced surface treatment of the initial HOPG surface, like etching, is recommended because it will produce a smoother initial HOPG surface than the manual cleaning procedure used in the current work. Based on the results presented in this thesis, the suggested cleaning procedure may be capable of more repeatedly producing thinner graphite layers containing fewer surface defects. The use of a higher (> 3000 Hz) shear oscillation frequency and varying the oscillation amplitude is recommended to see if further modification of these parameters enables the exfoliation of thinner graphite sheets including few-layer or mono-layer graphene. Also, as briefly discussed in Chapter 8, the PDMS stamp based mechanical exfoliation process on mesas or micro-pillars of HOPG should be investigated further to determine process conditions necessary to produce large area, thin graphite sheets. Better experimental design and understanding of the mesa-based approach is needed.

APPENDIX

Table A.1: Design of experiments results using three input factors to exfoliate large layer

Test No.	Contact Force	Dwell Time (min)	Speed (mm/s)	Exfoliated Surface Area (mm^2)
1	5	1	10	0.96
2	5	5	10	0.55
3	5	10	10	1.26
4	5	1	20	1.10
5	5	5	20	0.50
6	5	10	20	0.52
7	5	1	30	1.08
8	5	5	30	1.17
9	5	10	30	9.52
10	10	1	10	2.52
11	10	5	10	8.80
12	10	10	10	5.94
13	10	1	20	4.40
14	10	5	20	4.84
15	10	10	20	6.60
16	10	1	30	3.30
17	10	5	30	12.00
18	10	10	30	4.40
19	15	1	10	2.20
20	15	5	10	4.40
21	15	10	10	3.30
22	15	1	20	5.50
23	15	5	20	5.94
24	15	10	20	2.25
25	15	1	30	4.50
26	15	5	30	2.70
27	15	10	30	1.95

REFERENCES

[1] A. K. Geim and K. S. Novoselov, "The Rise of Graphene," *Nat. Mater.,* vol. 6, pp. 183-191, 2007.

[2] K. S. Novoselov, Z. Jiang, Y. Zhang, S. V. Morozov, H. L. Stormer, U. Zeitler*, et al.*, "Room-Temperature Quantum Hall Effect in Graphene," *Science,* vol. 315, pp. 1379-1379, 2007.

[3] K. S. Novoselov, V. I. Falko, L. Colombo, P. R. Gellert, M. G. Schwab, and K. Kim, "A Roadmap for Graphene," *Nature,* vol. 490, pp. 192-200, 2012.

[4] K. S. Novoselov, A. K. Geim, S. V. Morozov, D. Jiang, Y. Zhang, S. V. Dubonos*, et al.*, "Electric field effect in atomically thin carbon films," *Science,* vol. 306, pp. 666-9, Oct 22 2004.

[5] C. Reeves, "Graphene: Characterization After Mechanical Exfoliation," Senior, Physics, College of William and Mary, 2010.

[6] B. Z. Jang and A. Zhamu, "Processing of nanographene platelets (NGPs) and NGP nanocomposites: a review," *Journal of Materials Science,* vol. 43, pp. 5092-5101, 2008.

[7] H. Chang, G. Wang, A. Yang, X. Tao, X. Liu, Y. Shen*, et al.*, "A Transparent, Flexible, Low-Temperature, and Solution-Processible Graphene Composite Electrode," *Advanced Functional Materials,* vol. 20, pp. 2893-2902, 2010.

[8] R. Ruoff, "Graphene: Calling all chemists," *Nat Nano,* vol. 3, pp. 10-11, 2008.

[9] F. J. García de Abajo, "Graphene Plasmonics: Challenges and Opportunities," *ACS Photonics,* vol. 1, pp. 135-152, 2014/03/19 2014.

[10] C.-Y. Wen and G.-W. Huang, "Application of a thermally conductive pyrolytic graphite sheet to thermal management of a PEM fuel cell," *Journal of Power Sources,* vol. 178, pp. 132-140, 2008.

[11] (2015) Pyrolytic Graphite Sheet Evolves to Meet Tough Thermal Demands. *Electronic Design*. Available: http://electronicdesign.com/circuit-protection/pyrolytic-graphite-sheet-evolves-meet-tough-thermal-demands

[12] T. Yoichi, K. Sayuri, and S. Kuniaki, "Performance improvement of stacked graphite sheets for cooling applications," in *2008 58th Electronic Components and Technology Conference*, 2008, pp. 760-764.

[13] S. Z. Butler, S. M. Hollen, L. Cao, Y. Cui, J. A. Gupta, H. R. Gutiérrez*, et al.*, "Progress, Challenges, and Opportunities in Two-Dimensional Materials Beyond Graphene," *ACS Nano,* vol. 7, pp. 2898-2926, 2013/04/23 2013.

[14] M. Xu, T. Liang, M. Shi, and H. Chen, "Graphene-Like Two-Dimensional Materials," *Chemical Reviews,* vol. 113, pp. 3766-3798, 2013/05/08 2013.

[15] N. Krane, "Preparation of Graphene," Freie Universitat Berlin2011.

[16] S. Stankovich, D. A. Dikin, G. H. B. Dommett, K. M. Kohlhaas, E. J. Zimney, E. A. Stach*, et al.*, "Graphene-Based Composite Materials," *Nature,* vol. 442, pp. 282-286, 2006.

[17] M. J. Allen, V. C. Tung, and R. B. Kaner, "Honeycomb Carbon: A Review of Graphene," *Chemical Reviews,* vol. 110, pp. 132-145, 2009.

[18] R. A. P. B. Jayasena, "Few Layers of Graphene and Carbon Nanoscrolls by Wedge Based Mechanical Exfoliation," PhD Thesis, Nanyang Technological University, 2014.

[19] W. A. de Heer, C. Berger, X. Wu, P. N. First, E. H. Conrad, X. Li*, et al.*, "Epitaxial graphene," *Solid State Communications,* vol. 143, pp. 92-100, 2007.

[20] S. Bae, H. Kim, Y. Lee, X. Xu, J.-S. Park, Y. Zheng*, et al.*, "Roll-to-roll production of 30-inch graphene films for transparent electrodes," *Nat Nano,* vol. 5, pp. 574-578, 08//print 2010.

[21] K. S. Kim, Y. Zhao, H. Jang, S. Y. Lee, J. M. Kim, K. S. Kim*, et al.*, "Large-scale pattern growth of graphene films for stretchable transparent electrodes," *Nature,* vol. 457, pp. 706-710, 02/05/print 2009.

[22] S. C. O'Hern, C. A. Stewart, M. S. H. Boutilier, J.-C. Idrobo, S. Bhaviripudi, S. K. Das*, et al.*, "Selective Molecular Transport through Intrinsic Defects in a Single Layer of CVD Graphene," *ACS Nano,* vol. 6, pp. 10130-10138, 2012/11/27 2012.

[23] I. Janowska, O. Ersen, T. Jacob, P. Vennégues, D. Bégin, M.-J. Ledoux*, et al.*, "Catalytic unzipping of carbon nanotubes to few-layer graphene sheets under microwaves irradiation," *Applied Catalysis A: General,* vol. 371, pp. 22-30, 2009.

[24] T. Humberto, L. Ruitao, T. Mauricio, and S. D. Mildred, "The role of defects and doping in 2D graphene sheets and 1D nanoribbons," *Reports on Progress in Physics,* vol. 75, p. 062501, 2012.

[25] Z.-S. Wu, W. Ren, L. Gao, J. Zhao, Z. Chen, B. Liu*, et al.*, "Synthesis of Graphene Sheets with High Electrical Conductivity and Good Thermal Stability by Hydrogen Arc Discharge Exfoliation," *ACS Nano,* vol. 3, pp. 411-417, 2009.

[26] G. Sun, X. Li, Y. Qu, X. Wang, H. Yan, and Y. Zhang, "Preparation and characterization of graphite nanosheets from detonation technique," *Materials Letters,* vol. 62, pp. 703-706, 2008.

[27] J. Meihua, J. Hae-Kyung, K. Tae-Hyung, S. Kang Pyo, C. Yan, Y. Woo Jong*, et al.*, "Synthesis and systematic characterization of functionalized graphene sheets generated by thermal exfoliation at low temperature," *Journal of Physics D: Applied Physics,* vol. 43, p. 275402, 2010.

[28] D. Parobek, G. Shenoy, F. Zhou, Z. Peng, M. Ward, and H. Liu, "Synthesizing and Characterizing Graphene via Raman Spectroscopy: An Upper-Level Undergraduate Experiment That Exposes Students to Raman Spectroscopy and a 2D Nanomaterial," *Journal of Chemical Education,* vol. 93, pp. 1798-1803, 2016/10/11 2016.

[29] L. Xuekun, Y. Minfeng, H. Hui, and S. R. Rodney, "Tailoring graphite with the goal of achieving single sheets," *Nanotechnology,* vol. 10, p. 269, 1999.

[30] Y. B. Zhang, J. P. Small, W. V. Pontius, and P. Kim, "Fabrication and Electric-Field-Dependent Transport Measurements of Mesoscopic Graphite Devices," *Appl. Phys. Lett.,* vol. 86, pp. 073104-073107, 2005.

[31] B. Jayasena and S. Subbiah, "A novel mechanical cleavage method for synthesizing few layer graphenes," *Nanoscale Res. Lett.,* vol. 6, pp. 95-101, 2011.

[32] B. Jayasena, C. D. Reddy, and S. Subbiah, "Separation, Folding and Shearing of Graphene Layers During Wedge-Based Mechanical Exfoliation," *Nanotechnology,* vol. 24, pp. 205301-205308, 2013.

[33] A. Carlson, A. M. Bowen, Y. Huang, R. G. Nuzzo, and J. A. Rogers, "Transfer Printing Techniques for Materials Assembly and Micro/Nanodevice Fabrication," *Advanced Materials,* vol. 24, pp. 5284-5318, 2012.

[34] E. Menard and J. A. Rogers, "Stamping Techniques for Micro- and Nanofabrication," in *Springer Handbook of Nanotechnology*, B. Bhushan, Ed., ed Berlin, Heidelberg: Springer Berlin Heidelberg, 2010, pp. 313-332.

[35] H. Li, J. Wu, X. Huang, Z. Yin, J. Liu, and H. Zhang, "A Universal, Rapid Method for Clean Transfer of Nanostructures onto Various Substrates," *ACS Nano,* vol. 8, pp. 6563-6570, 2014/07/22 2014.
[36] M. A. Meitl, Z.-T. Zhu, V. Kumar, K. J. Lee, X. Feng, Y. Y. Huang*, et al.*, "Transfer printing by kinetic control of adhesion to an elastomeric stamp," *Nat Mater,* vol. 5, pp. 33-38, 01//print 2006.
[37] F. Hua, Y. Sun, A. Gaur, M. A. Meitl, L. Bilhaut, L. Rotkina*, et al.*, "Polymer Imprint Lithography with Molecular-Scale Resolution," *Nano Letters,* vol. 4, pp. 2467-2471, 2004/12/01 2004.
[38] K. Yoo, S. Takei Y Fau - Kim, S. Kim S Fau - Chiashi, S. Chiashi S Fau - Maruyama, K. Maruyama S Fau - Matsumoto, I. Matsumoto K Fau - Shimoyama*, et al.*, "Direct physical exfoliation of few-layer graphene from graphite grown on a nickel foil using polydimethylsiloxane with tunable elasticity and adhesion," 20130423 DCOM- 20131104.
[39] Y. Lee, S. Bae, H. Jang, S. Jang, S.-E. Zhu, S. H. Sim*, et al.*, "Wafer-Scale Synthesis and Transfer of Graphene Films," *Nano Letters,* vol. 10, pp. 490-493, 2010/02/10 2010.
[40] M. J. Allen, V. C. Tung, L. Gomez, Z. Xu, L.-M. Chen, K. S. Nelson*, et al.*, "Soft Transfer Printing of Chemically Converted Graphene," *Advanced Materials,* vol. 21, pp. 2098-2102, 2009.
[41] X. Lu, H. Huang, N. Nemchuk, and R. S. Ruoff, "Patterning of highly oriented pyrolytic graphite by oxygen plasma etching," *Applied Physics Letters,* vol. 75, pp. 193-195, 1999.
[42] D. Li, W. Windl, and N. P. Padture, "Toward Site-Specific Stamping of Graphene," *Advanced Materials,* vol. 21, pp. 1243-1246, 2009.
[43] C. Chun-Hu, M. R. Kongara, and P. P. Nitin, "Site-specific stamping of graphene micro-patterns over large areas using flexible stamps," *Nanotechnology,* vol. 23, p. 235603, 2012.
[44] J. Butikova, B. Polyakov, L. Dimitrocenko, E. Butanovs, and I. Tale, "Laser scribing on HOPG for graphene stamp printing on silicon wafer," *Central European Journal of Physics,* vol. 11, pp. 580-583, 2013// 2013.
[45] S. Goler, V. Piazza, S. Roddaro, V. Pellegrini, F. Beltram, and P. Pingue, "Self-assembly and electron-beam-induced direct etching of suspended graphene nanostructures," *Journal of Applied Physics,* vol. 110, p. 064308, 2011.
[46] M. Yi and Z. Shen, "A review on mechanical exfoliation for the scalable production of graphene," *Journal of Materials Chemistry A,* vol. 3, pp. 11700-11715, 2015.
[47] B. Jayasena and S. Melkote, "An Investigation of PDMS stamp assisted mechanical exfoliation of large area graphene," in *Proceedings of the North American Manufacturing* Charlotte, 2015.
[48] J. S. Park, A. Reina, R. Saito, J. Kong, G. Dresselhaus, and M. S. Dresselhaus, "band Raman spectra of single, double and triple layer graphene," *Carbon,* vol. 47, pp. 1303-1310, 4// 2009.
[49] Z. H. Ni, H. M. Wang, J. Kasim, H. M. Fan, T. Yu, Y. H. Wu*, et al.*, "Graphene Thickness Determination Using Reflection and Contrast Spectroscopy," *Nano Letters,* vol. 7, pp. 2758-2763, 2007/09/01 2007.
[50] M. L. B. Guilhem Velvé Casquillas, Emmanuel Terriac, Fabien Bertholle, Timothée Houssin and Sebastien Cargou. HOW TO DO A SPIN-COATED PDMS LAYER? – APPLICATION NOTE. *PDMS MEMBRANE: THICKNESS OF A SPIN COATED PDMS LAYER*. Available: http://www.elveflow.com/microfluidic-tutorials/soft-lithography-

reviews-and-tutorials/introduction-in-soft-lithography/pdms-membrane-thickness-of-a-spin-coated-pdms-layer/
[51] M. Wall, "Raman Spectroscopy," *Advanced Materials & Processes,* vol. 170, pp. 35-38, 2012.
[52] M. B. Heaney, Ed., *Electrical Conductivity and Resistivity* (Electrical Measurement, Signal Processing, and Displays. CRC Press, 2003, p.^pp. Pages.
[53] F. M. Smits, "Measurement of Sheet Resistivities with the Four-Point Probe," *Bell System Technical Journal,* vol. 37, pp. 711-718, 1958.
[54] D. K. Schroder. (2006). *Semiconductor Material and Device Characterization.*
[55] A. J. Schmidt, X. Chen, and G. Chen, "Pulse accumulation, radial heat conduction, and anisotropic thermal conductivity in pump-probe transient thermoreflectance," *Review of Scientific Instruments,* vol. 79, p. 114902, 2008.
[56] D. G. Cahill, "Analysis of heat flow in layered structures for time-domain thermoreflectance," *Review of Scientific Instruments,* vol. 75, pp. 5119-5122, 2004.
[57] T. L. Bougher, L. Yates, C.-F. Lo, W. Johnson, S. Graham, and B. A. Cola, "Thermal Boundary Resistance in GaN Films Measured by Time Domain Thermoreflectance with Robust Monte Carlo Uncertainty Estimation," *Nanoscale and Microscale Thermophysical Engineering,* vol. 20, pp. 22-32, 2016/01/02 2016.
[58] , ed: SPI Supplies.
[59] Y. Wang, D. C. Alsmeyer, and R. L. McCreery, "Raman spectroscopy of carbon materials: structural basis of observed spectra," *Chemistry of Materials,* vol. 2, pp. 557-563, 1990/09/01 1990.